Cell, Vol. 113, 905–917, June 27, 2003, Copyright ©2003 by Cell Press

The Chromatin-Remodeling Complex WINAC Targets a Nuclear Receptor to Promoters and Is Impaired in Williams Syndrome

Hirochika Kitagawa,[1,2] Ryoji Fujiki,[1]
Kimihiro Yoshimura,[1] Yoshihiro Mezaki,[1]
Yoshikatsu Uematsu,[1] Daisuke Matsui,[1]
Satoko Ogawa,[1] Kiyoe Unno,[1,3] Mataichi Okubo,[3]
Akifumi Tokita,[3] Takeya Nakagawa,[4]
Takashi Ito,[4] Yukio Ishimi,[5]
Hiromichi Nagasawa,[6] Toshio Matsumoto,[2]
Junn Yanagisawa,[1,7] and Shigeaki Kato[1,7,*]
[1]Institute of Molecular and Cellular Biosciences
University of Tokyo
1-1-1 Yayoi
Bunkyo-ku
Tokyo 113-0032
Japan
[2]First Department of Internal Medicine
University of Tokushima School of Medicine
3-18-15 Kuramoto-cho
Tokushima 770-8503
Japan
[3]Department of Pediatrics
Juntendo University School of Medicine
3-1-3 Hongo
Bunkyo-ku
Tokyo 113-8431
Japan
[4]Department of Biochemistry
Nagasaki University School of Medicine
1-12-4 Sakamoto
Nagasaki 852-8523
Japan
[5]Mitsubishi Kagaku Institute of Life Sciences
11 Minamiooya
Machida-shi
Tokyo 194-8511
Japan
[6]Department of Applied Biological Chemistry
Graduate School of Agricultural and Life Sciences
University of Tokyo
1-1-1 Yayoi
Bunkyo-ku
Tokyo 113-0032
Japan
[7]SORST
Japan Science and Technology
4-1-8 Honcho
Kawaguchi
Saitama 332-0012
Japan

Summary

We identified a human multiprotein complex (WINAC) that directly interacts with the vitamin D receptor (VDR) through the Williams syndrome transcription factor (WSTF). WINAC has ATP-dependent chromatin-remodeling activity and contains both SWI/SNF components and DNA replication-related factors. The latter might explain a WINAC requirement for normal S phase progression. WINAC mediates the recruitment of unliganded VDR to VDR target sites in promoters, while subsequent binding of coregulators requires ligand binding. This recruitment order exemplifies that an interaction of a sequence-specific regulator with a chromatin-remodeling complex can organize nucleosomal arrays at specific local sites in order to make promoters accessible for coregulators. Furthermore, overexpression of WSTF could restore the impaired recruitment of VDR to vitamin D regulated promoters in fibroblasts from Williams syndrome patients. This suggests that WINAC dysfunction contributes to Williams syndrome, which could therefore be considered, at least in part, a chromatin-remodeling factor disease.

*Corresponding author: uskato@mail.ecc.u-tokyo.ac.jp

Introduction

Lipophilic ligands, such as fat-soluble vitamins A/D and thyroid/steroid hormones, exert their actions through transcriptional control of particular sets of target genes by direct binding and consequent activation of their cognate nuclear receptors (NRs) (Mangelsdorf et al., 1995). NRs form a superfamily and act as ligand-inducible regulators. From their functional and structural similarities, NR proteins are divided into five functional domains, designated A to E. The ligand binding domain (LBD) is located in the C-terminal E domain. The most conserved domain, C, is located in the NR center and serves as the DNA binding domain to specifically recognize and directly bind to their cognate ligand response elements in the target promoters. The LBD also harbors ligand-inducible transactivation function (AF-2). Upon ligand binding, NRs control transcription through ligand-dependent associations with a number of coregulators and coregulator complexes (Glass and Rosenfeld, 2000).

At transcriptional initiation sites in promoters, distinct classes of multiprotein complexes are thought to be indispensable for controlling transcription of sequence-specific regulators (Emerson, 2002; Narlikar et al., 2002). These complexes modify the chromatin configuration in a highly regulated manner, like nucleosome rearrangement, and bridge the functions between regulators and basal transcription factors, along with RNA polymerase II. Two major classes of chromatin-modifying complexes have been well characterized and their anchoring to the promoters presumably requires enzyme-catalyzed modifications of histone tails in chromatin (Hassan et al., 2002). One class contains several discrete subfamilies of transcription coregulatory complexes with either histone acetylase (HAT) or histone deacetylase (HDAC) activities to covalently modify histones through acetylation. In NR

ligand-induced transactivation processes, the complexes containing HDAC first act to corepress transactivation of unliganded NRs, while upon ligand binding, two HAT complexes, p160/CBP and TRRAP/GCN5, coactivate the NR function, like the other non-HAT DRIP/TRAP/SMCC coactivator complexes (Onate et al., 1995; Kamei et al., 1996; Rachez et al., 1998; Gu et al., 1999; Yanagisawa et al., 2002).

Another class of complexes uses ATP hydrolysis to rearrange nucleosomal arrays in a noncovalent manner and render chromosomal DNA accessible for sequence-specific regulators (Narlikar et al., 2002). These ATP-dependent chromatin-remodeling complexes act on transcription, DNA repair, and DNA replication and have been classified into subfamilies based on the major catalytic components with ATPase activity, SWI2/SNF2, ISWI, and Mi-2 (Fyodorov and Kadonaga, 2001; Yasui et al., 2002). These ATPases are highly conserved from yeast to humans and each forms a functionally similar, but distinct complex with a combination of specific components. However, the roles of most of the other components, except the catalytic subunits in chromatin remodeling, remain largely unknown (Narlikar et al., 2002).

Accumulating evidence revealed that both the chromatin-remodeling complexes and the coregulatory complexes cooperatively support transactivation of sequence-specific regulators like NRs (Glass and Rosenfeld, 2000; Emerson, 2002; Narlikar et al., 2002). However, the underlying molecular basis of the functional interplay among the complexes and the order of their recruitment through regulators to the promoters in controlling transcription at the specific local sites on the promoters are largely unknown.

Williams syndrome (WS) is a rare autosomal dominant hereditary disorder with multiple symptoms, including typically congenital vascular lesion, elfin face, mental retardation, and growth deficiency (Lu et al., 1998). Transient appearance of infantile aberrant vitamin D metabolism and hypercalcemia in the WS patients was also documented (Taylor et al., 1982; Garabedian et al., 1985). This syndrome is associated with genetic deletions at chromosome 7q 11.23, and several candidate genes in the deleted regions have been mapped from their mRNA expression levels (Hoogenraad et al., 2002). One gene, the Williams syndrome transcription factor (WSTF), has been suspected to be a candidate responsible for the diverse WS disorders (Lu et al., 1998; Peoples et al., 1998). This possibility is raised by the fact that WSTF is highly homologous to hACF1 as one of the WAC family proteins (Jones et al., 2000). Also, hACF1 is a partner of hSNF2h (a *Drosophila* ISWI homolog) to form well-characterized ISWI-based chromatin-remodeling complexes (Poot et al., 2000).

To search a chromatin-modifying complex to account for the ligand-independent occupancy of VDR in the target promoters, we purified from MCF7 cells a human multiprotein complex named "WINAC". The analysis of WINAC represents not only a molecular mechanism that a direct and selective interaction of a sequence-specific regulator with a chromatin-remodeling complex, but also the relationship between the function of WINAC and Williams syndrome disorders.

Results

Purification of a WSTF-Containing Multiprotein Complex Interacting with the VDR Ligand Binding Domain

To identify a coregulator complex for nuclear receptors, HeLa cell nuclear extracts were incubated with a chimeric VDR-DEF region protein (VDR-DEF) fused to glutathione-S-transferase (GST), in the presence or absence of 1α,25(OH)2D3 (Figure 1A). Proteins associated with VDR were collected under a milder washing condition (Yanagisawa et al. 2002) than that in the previous report (Rachez et al., 1998). Proteins that interacted with VDR-DEF were separated by SDS-PAGE and silver stained (Figure 1B). Mass spectrometry and the apparent molecular weights of the different proteins associated with the VDR-DEF in a ligand-dependent way led to the identification of several known components of the DRIP/TRAP/SMCC complex (Figure 1B), in agreement with previous observations (Rachez et al., 1998; Gu et al., 1999; Yanagisawa et al., 2002). One of the ligand-independent VDR-specific interactants was the Williams syndrome transcription factor (WSTF)/WBSCR9/BAZ1B (Lu et al., 1998; Peoples et al., 1998; Jones et al., 2000) (Figure 1B), and the WSTF protein was detected indeed in native HeLa cells (Figure 1C).

By Western blotting with specific antibodies, the NR coactivators, TRAP220 and TIF2, were detected only when VDR and ERα were liganded (Figure 1B). Unlike these factors, no ligand dependency, but VDR-selective interaction was found in WSTF (Figure 1B). By a GST pull-down assay, the physical and constitutive interaction of recombinant WSTF in vitro was observed for VDR-DEF irrespective of ligand binding, but not detected for ERα LBD (Figure 1D). In coimmunoprecipitations using the nuclear extracts of transfected MCF7 cells, WSTF appeared to interact with both unliganded and liganded VDR, while ligand-dependent recruitment of TRAP220 and TIF2 were expectedly seen for VDR as well as ERα (Yanagisawa et al., 2002) (Figure 1E).

To purify a WSTF-containing complex, we established a MCF7 stable transformant overexpressing FLAG-tagged WSTF. With the nuclear extracts of the stable transformants, WSTF containing complexes were isolated by multistep purification using the GST-VDR column and an anti-FLAG affinity resin column (Figure 2A). On the glycerol density gradient (Figure 2B, upper image), the purified complexes with a molecular weight of greater than 670 kDa bound to the GST-VDR column and these large molecular weight fractions contained WSTF, indicating that WSTF forms a stable nuclear complex. The fractions containing FLAG-tagged WSTF were then applied on the anti-FLAG affinity column to isolate the complex.

Identification of a WSTF Complex

With the mass fingerprinting, we identified all the components of the purified complex containing WSTF (Figure 2C), and designated this complex as WINAC (*W*STF *I*ncluding *N*ucleosome *A*ssembly *C*omplex). WINAC stable formation was further supported by coimmunoprecipitation with a CAF-1p150 antibody (Figure 2C). WINAC consists of at least 13 components, but unexpectedly

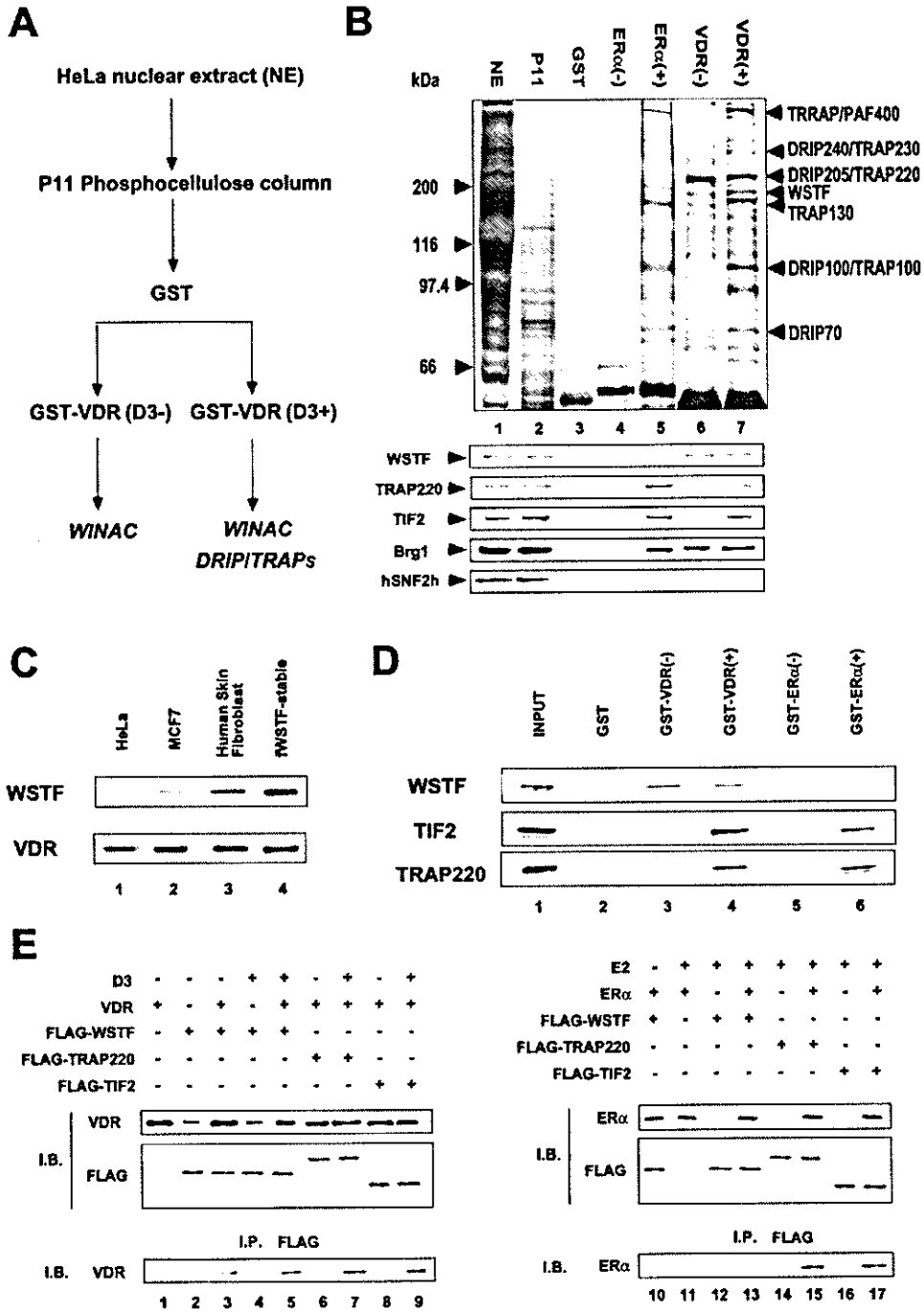

Figure 1. Purification and Identification of Human Proteins Interacting with 1α,25(OH)2D3, Unbound and Bound VDR

(A) Purification scheme for VDR interacting proteins. The eluted fraction from P11 phosphocellulose column was incubated with immobilized GST-VDR(DEF) in the absence or presence of 1α,25(OH)2D3(D3,10^{-6} M).

(B) Identification of ligand-independent and -dependent VDR interacting proteins. In the upper image, fractions were subjected to SDS-PAGE, followed by silver staining. Total HeLa S3 nuclear extract [NE] (lane 1), a fraction eluted from the P11 column [p11] (lane 2), fractions from GST [GST] (lane 3), unliganded- and liganded-GST-ERα(DEF) columns [ERα(−);ERα(+)] (lanes 4 and 5), unliganded- and liganded-GST-VDR(DEF) columns [VDR(−);VDR(+)] were examined by mass spectrometry and identified proteins are indicated at the right side of the image. The lower image shows Western blot analysis using specific antibodies shown in the image.

(C) Protein expression in cultured cells. Western blotting with antibodies against WSTF or VDR was performed with indicated cell lines (3 × 10^6 cells/lane).

(D) Direct and ligand-independent interaction of WSTF with VDR in vitro. WSTF, TIF2, and TRAP220 were translated in vitro and incubated with a receptor-GST chimeric protein immobilized on glutathione-Sepharose beads in the presence or absence of the cognate ligands.

(E) 1α,25(OH)2D3-independent interaction between VDR and WSTF in vivo. The upper image displays the Western blot of the total cell extracts (Yanagisawa et al., 2002) to verify expression. The lower image shows the Western blot of the immunoprecipitates by anti-FLAG M2-affinity resin to detect the receptor.

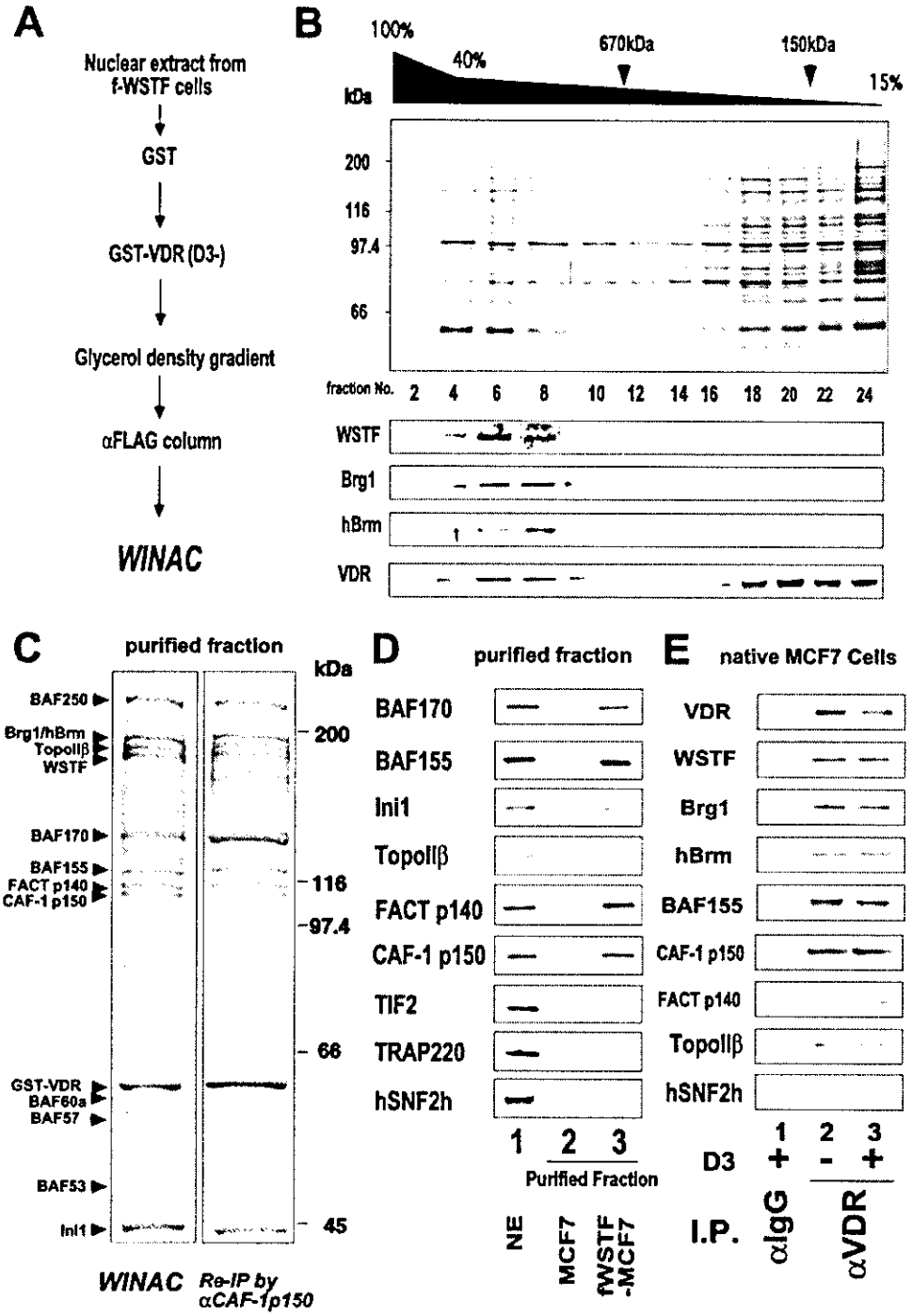

Figure 2. Purification and Identification of a Human WSTF-Containing Multiprotein Complex "WINAC"

(A) Purification scheme of WINAC from MCF7 stable transformants (Yanagisawa et al., 2002).

(B) Fractionation of purified complexes on glycerol density gradient. In the lower image, Western blot analysis of each fraction using specific antibodies is shown.

(C) The purified complex was subjected to SDS-PAGE, followed by silver staining and identified by mass spectrometry (left image). The right image shows the reimmunoprecipitation (Re-IP) of purified WINAC by the anti-CAF-1 p150 antibody.

(D) Western blot analysis of WINAC. Western blot analysis was performed to compare nuclear extracts (lane 1), mock MCF7 (lane 2), and FLAG-WSTF stable transformants containing WINAC (lane 3) with specific antibodies.

(E) Detection of endogenous WINAC components by Western blotting.

contains neither hSNF2h nor the components of known ISWI-based complexes (Figure 2C). Rather, the SWI/SNF type ATPases (Brg1 and hBrm) and several BAF components share with the SWI2/SNF2-based complexes (Narlikar et al., 2002). However, we could not detect BAF180, which is specific to one of the hSWI/

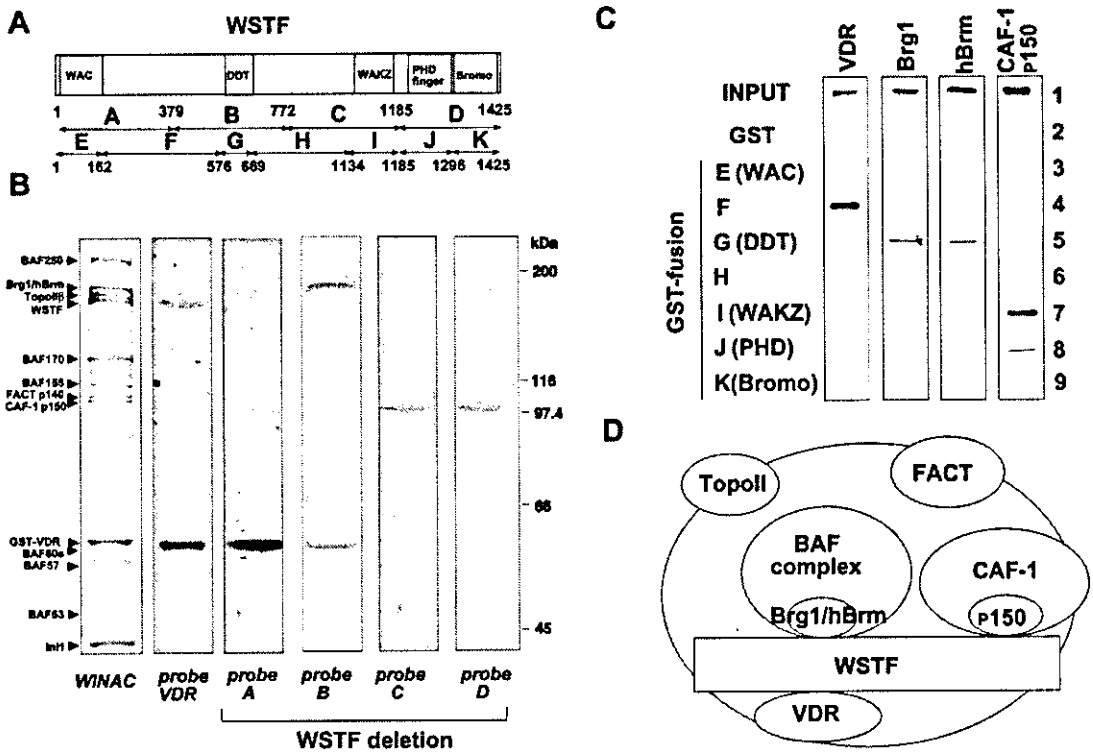

Figure 3. WSTF as a Platform Protein in WINAC

(A) Schematic representation of the probes used for the Far Western blotting and the GST pull-down assay. WSTF deletion mutants are expressed as GST-chimeric proteins.

(B) Far Western blotting of the WINAC complex probed with indicated ^{32}P-labeled GST-fused chimeric proteins. ^{32}P-labeled GST-fused chimeric proteins were prepared with pGEX-2TK vector (Amersham Biosciences) by PKA phosphorylation (Rachez et al., 1998).

(C) Physical interaction of WINAC components and VDR with WSTF deletion mutants in GST pull-down assay.

(D) Schematic representation of the interacting domains of WSTF.

SNF-type complexes, PBAF, which was purified and identified by in vitro transcription to coactivate VDR in a ligand-dependent manner (Lemon et al., 2001). Interestingly, WINAC appears to harbor three components (TopoIIβ, FACTp140, and CAF-1p150) (Smith and Stillman, 1989; Varga-Weisz et al., 1997; LeRoy et al., 1998), which have not yet been found in any known ATP-dependent chromatin-remodeling complexes. Western blotting with specific antibodies verified several WINAC components (Figure 2D). Moreover, major WINAC components in a purified endogenous complex associating with VDR were detected (Figure 2E), supporting presence of WINAC as a stable complex in native cells.

Clear retention of VDR was detected upon the WSTF band, but not the other subunits (Figure 3B), confirming the GST-pull-down assay results (Figure 1D). The WSTF fragments were trapped on not only VDR but also CAF-1p150 and Brg1/hBrm (Figure 3B). Such interactions were also seen in the expected regions by the GST-pull-down assay (Figure 3C), suggesting that WSTF serves as a platform subunit to assemble components into WINAC (as illustrated in Figure 3D).

WINAC Is a Multifunctional ATP-Dependent Chromatin-Remodeling Complex

We then examined if purified WINAC exerts an ATP-dependent chromatin-remodeling activity by comparing its activity with a complex of the recombinant dAcf1 and dISWI proteins in a standard micrococcal nuclease assay. This recombinant complex has been reported sufficient to mobilize nucleosomes in vitro in an ATP-dependent manner (Ito et al., 1997). Like the dISWI complex, an ATP-dependent chromatin-assembly reaction was clearly induced by WINAC (compare lanes 6, 7, and lane 3 in Figure 4A), indicating that Brg1/hBrm in WINAC serves as an ATPase for this ATP-dependent chromatin-remodeling process. WINAC appeared to have a chromatin-assembly activity (data not shown) like RSF (Loyola et al., 2001).

We then examined the ability of WINAC to disrupt nucleosome arrays through VDR bound DNA since the known ATP-dependent chromatin-remodeling complexes are potent to recognize the nucleosomal array around the binding sites of a sequence-specific regulator (Ito et al., 1997; Lemon et al., 2001). By Southern blot analysis with a pair of oligonucleotides complementary to a region in the vicinity (promoter probe) or to a site about 900 bp upstream (distal probe) of the GAL4 DBD binding sites for a chimeric VDR-DEF protein (GAL-VDR), disruption of the nucleosome arrays in the GAL4 binding site vicinity was induced only when both VDR and WINAC were present (lane 4 in Figure 4B), while the other regions appeared unaffected in the nucleosome arrays (Figure 4B). Reflecting the VDR-specific nucleo-

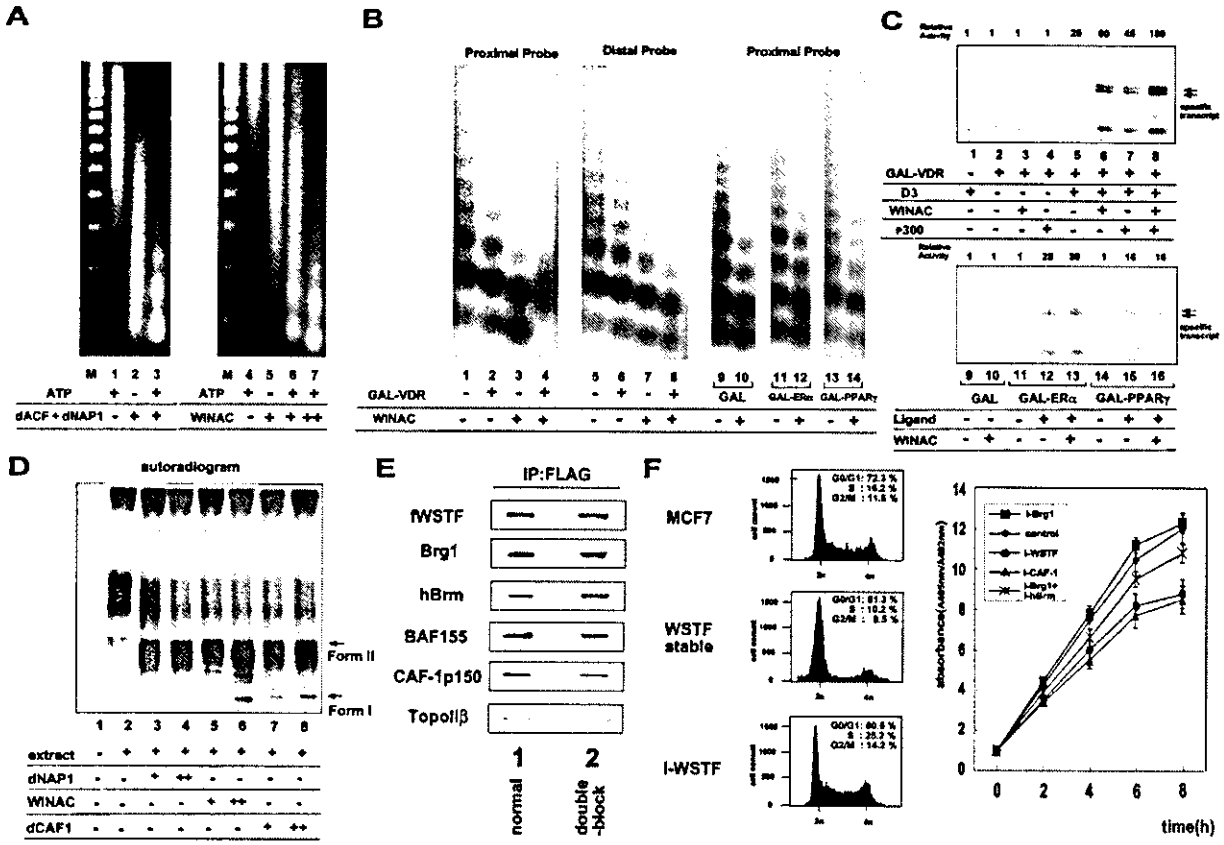

Figure 4. WINAC as an ATP-Dependent Chromatin-Remodeling Complex

(A) Chromatin-reconstitution activity of WINAC. The reacted samples were subjected to partial micrococcal nuclease digestion. The molecular mass marker (M) is the 200 bp ladder.

(B) Chromatin disruption by WINAC is specifically VDR dependent. Oligonucleotide probe corresponds to either a sequence between the GAL4 sites and the RNA start site (proximal probe) or 900 bp upstream of the start site (distal probe).

(C) Potentiation of VDR transactivation by WINAC in vitro. Arrows indicate specific transcripts by transcription reactions by GAL4 derivatives. A representative result is displayed, and relative activities were calculated from three independent assays with pGI0 vector as an internal control.

(D) WINAC functions as a chromatin-reconstitution factor during DNA replication in vitro. During DNA replication induced by SV40 T antigen in vitro, WINAC could form chromatin with negatively supercoiled DNA. Form I, a perfect supercoiled DNA; form II, a relaxed form.

(E) WINAC formation is unchanged in S phase. MCF7 stable transformants were cultured under either normal conditions or double-thymidine block treatments.

(F) Modulation of the cell cycle by altered WSTF expression. Left image: DNA histogram of the MCF7 cells [MCF7], WSTF stably expressing MCF7 cells [WSTF stable] and MCF7 cells transfected with WSTF-RNAi [i-WSTF]. Right image: BrdU incorporation during S phase of the MCF7 cells transfected with RNAi from the indicated proteins during double-thymidine treatment. After the final release (time 0), cells were collected every 2 hr, for up to 8 hr. The average values of triplicate analyses are shown.

some disruption by WINAC among tested receptors (Figure 4B), ligand-induced transactivation in vitro was potentiated by WINAC for VDR, but for neither ERα nor PPARγ (Figure 4C).

WINAC Function during DNA Replication

The WINAC function in DNA replication (Smith and Stillman, 1989; Varga-Weisz et al., 1997) was addressed by reconstituting chromatin structure upon newly replicated DNA by an in vitro assay. WINAC, like the reported CAF-1 histone chaperone complex (see lanes 7 and 8 in Figure 4D), could facilitate forming chromatin structure with negatively supercoiled DNA on newly replicated DNA through nucleosome arrangement (Smith and Stillman, 1989) (Figure 4D). Moreover, WINAC complex formation was detected irrespective of the cell-cycle stages, even when blocked at S stage by double-thymidine treatments (Fujita et al., 1996) (Figure 4E). Manipulation of WSTF expression by WSTF-RNAi expression (Elbashir et al., 2001) resulted in alterations in the cell cycle (left images in Figure 4F). Particularly, DNA synthesis was clearly lowered by RNAi expression of either WSTF or Brg1/hBrm ATPases (right image in Figure 4F). Thus, these findings suggest that WINAC plays a role in chromatin remodeling during DNA replication.

WSTF Coactivated Ligand-Induced Transactivation Function of VDR

Next, we investigated if WSTF potentiates the ligand-induced transactivation of VDR in MCF7 cells by transient expression analysis. 1α,25(OH)2D3 (10^{-9} M) was effective to induce VDR AF-2 transactivation function.

WSTF coactivated this ligand-induced AF-2 function of VDR, but not ERα (compare lanes 3 and 4 with 23 and 24 in Figure 5A). Both Brg1 and hBrm were potent to enhance the transactivation functions of VDR and ERα (compare lanes 9 and 12 with lane 2 for VDR; lanes 29 and 32 with lane 22 for ERα in Figure 5A) as previously reported (Chiba et al., 1994; DiRenzo et al., 2000; Shang et al., 2000; Belandia et al., 2002). Interestingly, such coactivator-like activity of WSTF was selective for VDR, and not detected for ERα, even in the presence of Brg1/hBrm (see lanes 30 and 33 in Figure 5A).

To confirm such a coactivator-like function of WSTF for VDR, the ligand-induced transactivation function of VDR was assessed 40 hr after the RNAi transfection and was severely attenuated nearly to basal transcription levels (lanes 7 and 8 in Figure 5A). Interestingly, WSTF-RNAi expression was found to also abrogate the VDR coactivation of the VDR transcriptional activity by the known NR coactivators, such as TRAP220 and TIF2 (lanes 16 and 18 in Figure 5A). Similarly, RNAi expression resulted in a loss of the coactivator-like function of WSTF for VDR when intact VDR/RXR heterodimer was bound to a naturally occurring positive vitamin D response element (VDRE) derived from the human 1α,25-dihydroxyvitamin D3 24-hydroxylase [24(OH)ase] gene promoter (Chen and DeLuca, 1995) (Figure 5C). ChIP analysis revealed that VDR and the WINAC components were constitutively associated with the promoter irrespective of ligand binding. In the contrast, ligand-induced occupancy in the promoter was seen in TRAP220 and TIF2 with ligand-induced histone H4 acetylation (compare lane 3 with 4 in Figure 5B), though the ligand-induced TRAP220 and TIF2 occupancy was cyclic (data not shown) as expected from previous reports (Shang et al., 2000). Such ligand-dependent and -independent recruitments of factors to the promoter were robustly attenuated by WSTF-RNAi expression (lane 5 in Figure 5B).

As the VDR/RXR heterodimer also represses transcription in a ligand-dependent manner through negative VDRE (nVDRE), the action of WSTF in the ligand-induced transrepression was examined in a naturally occurring nVDRE in human 25-hydroxyvitamin D3 1α-hydroxylase [1α(OH)ase] (Murayama et al., 1998). ChIP analysis uncovered that VDR and WINAC appear to land on the nVDRE in a ligand-independent manner, while ligand-induced (compare lane 8 with 9 in Figure 5B), but cyclic (data not shown) recruitments of N-CoR and HDAC2 were observed. Ligand-dependent repression was exaggerated by WSTF overexpression (lanes 3 and 4 in Figure 5D), but attenuated again by WSTF-RNAi expression (lanes 5 and 6 in Figure 5D). Thus, it is likely that WINAC association with VDR facilitates targeting of a putative corepressor complex to the nVDRE. The WINAC function in the native VDR target gene promoters and the endogenous gene expressions of 24(OH)ase and 1α(OH)ase were further confirmed by the impaired 1α,25(OH)2D3 responsiveness by the WSTF ablation (Figure 5E). Thus, these findings point out that WINAC rearranges the nucleosome array around the positive and negative VDREs, thereby facilitating the coregulatory complexes accessible to VDR for further transcription control.

Impaired Transactivation Function of VDR Was Recovered by WSTF Overexpression in Williams Syndrome Patients

Together with these observations, the typical phenotypes of the WSTF gene-deleted WS patients (Taylor et al., 1982; Garabedian et al., 1985) prompted us to assume that a lowered WINAC function caused by reduced WSTF expression may result in aberrant chromatin remodeling, leading to diverse abnormalities, including abnormal vitamin D metabolism and hypercalcemia. Considering WSTF and VDR skin expression (Yoshizawa et al., 1997), we first assessed the ligand-induced transactivation function of VDR in skin fibroblast cells derived from three normal and three WS patients, in which the region covering the WSTF gene is deleted in one chromosome 7 allele, as representatively shown in patient #1 by FISH analysis (Figure 6A). Northern blot analysis unmasked the WSTF expression levels were clearly lowered (~50%) in the WS patients (Figure 6B). By a transient transfection assay in fibroblast cells, we found reduced transactivation function of VDR in the WS patient cells (Figure 6C). Consistent with the impaired function of VDR in the WS cells, the ChIP analysis showed robust reduction in targeting of VDR, the WINAC components, and the coactivators to the 24(OH)ase VDRE (lanes 9 and 10 in Figure 6E), in agreement with the MCF7 cell results (Figure 5B).

Most strikingly, WSTF expression by an adenovirus vector (Kitagawa et al., 2002) could rescue the reduced responsiveness of 24(OH)ase gene induction by 1α,25(OH)2D3 for 12 hr in the WS skin fibroblasts (compare lane 3 with 4 in Figure 6D), with the impaired promoter targeting of the WINAC components and unliganded recoveries in VDR to the 24(OH)ase promoter (see lane 11 in Figure 6E), and the impaired ligand-induced recruitment of the NR coactivators (see lane 12 in Figure 6). Thus, these findings suggest that at least a part of the endocrine disorders found in the WS patients are related to VDR malfunction caused by the lowered WINAC function, which is due to lower WSTF expression.

The WSTF transcript during embryogenesis was not detected by Northern blotting, but detectable by RT-PCR (Figure 7A). By whole mount in situ staining (Sekine et al., 1999) at 9.5 dpc, the WSTF transcript appeared to be ubiquitously expressed (data not shown), but its expression pattern became limited and partially overlapped with mouse Brg1 and BAF155 (Srg3) expression (Bultman et al., 2000; Kim et al., 2001) as evident at 11.5 dpc (Figure 7B). Surprisingly these expression patterns seem different from that of mouse Snf2h (Lazzaro and Picketts, 2001), particularly at brain. These results may suggest a specific role of WINAC during embryogenesis, which may account for the diverse abnormalities in the WS patients.

Discussion

Purification and Identification of a Human Multiprotein Complex Containing WSTF, WINAC

WINAC contains known components of the hSWI/SNF-type complexes, including two major ATPase subunits, Brg1 and hBrm (Figure 2C). However, by our purification

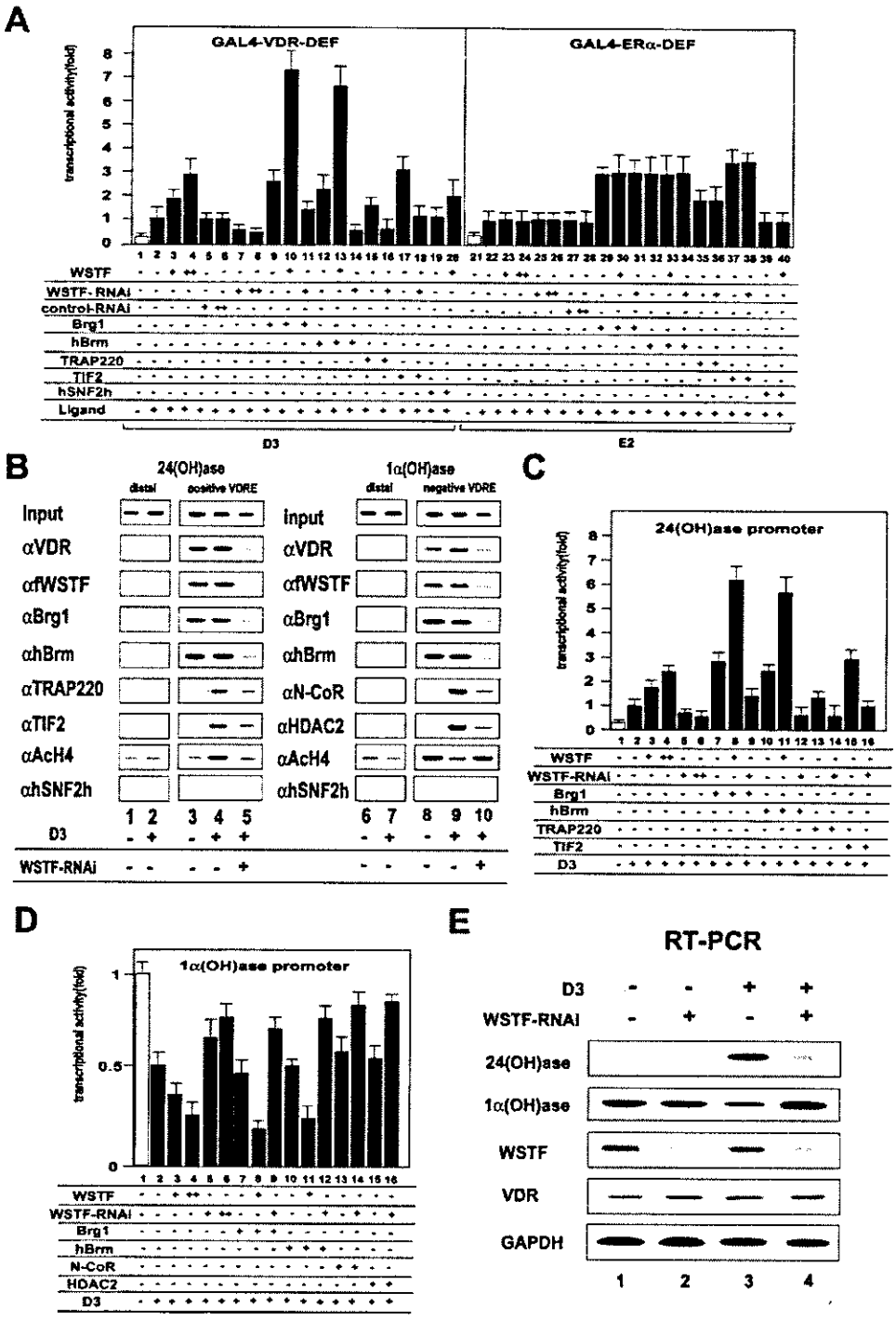

Figure 5. Ligand-Dependent Promoter Targeting of Coregulators through WINAC-VDR Association

(A) VDR-specific facilitation of co-activator accessibility by WINAC. MCF7 cells were transfected with the expression vectors of a luciferase reporter plasmid containing the GAL4 upstream activation sequence (UAS) [17mer(×2)] driven by the β-globin promoter (0.5 μg). PML-CMV (2 ng); GAL4-DBD-VDR-DEF (0.2 μg); GAL4-DBD-ERα DEF (0.2 μg); pDNA3-FLAG-WSTF (+; 0.1 μg: ++; 0.3 μg); pSV-Brg1 (0.2 μg); pSV-hBrm (0.2 μg); pcDNA3-TRAP220 (0.3 μg); pcDNA3-TIF2 (0.3 μg); siRNA (+; 0.1 μg: ++; 0.2 μg) of WSTF-RNAi; or control RNAi or their combinations were transfected as indicated in the images in the absence or presence of ligand (10^{-9} M). Bars in each graph show the fold change in luciferase activity relative to the activity of the receptor transactivation in the presence of ligand.

(B) ChIP analysis on the 24(OH)ase promoter and 1α(OH)ase promoter of WSTF stable transformants. Soluble chromatin was prepared from WSTF stable transformants treated with D3 (10^{-9} M) for 45 min and immunoprecipitated with indicated antibodies.

(C and D) The coregulator-like actions of WSTF on the naturally occurring positive and negative vitamin D response elements. MCF7 cells were transfected with the expression vectors of either the luciferase reporter plasmid containing a human 24(OH)ase promoter harboring a canonical positive VDRE or a human 1α(OH)ase promoter containing a negative VDRE and the factors shown in (A) or together with pcDNA3-N-CoR (0.3 μg), pcDNA3-HDAC2 (0.3 μg).

(E) WSTF-mediated regulations of endogenous genes by VDR. RT-PCR analysis of MCF7 cells was performed 12 hr after the induction by D3 (10^{-9} M) (Yanagisawa et al., 2002).

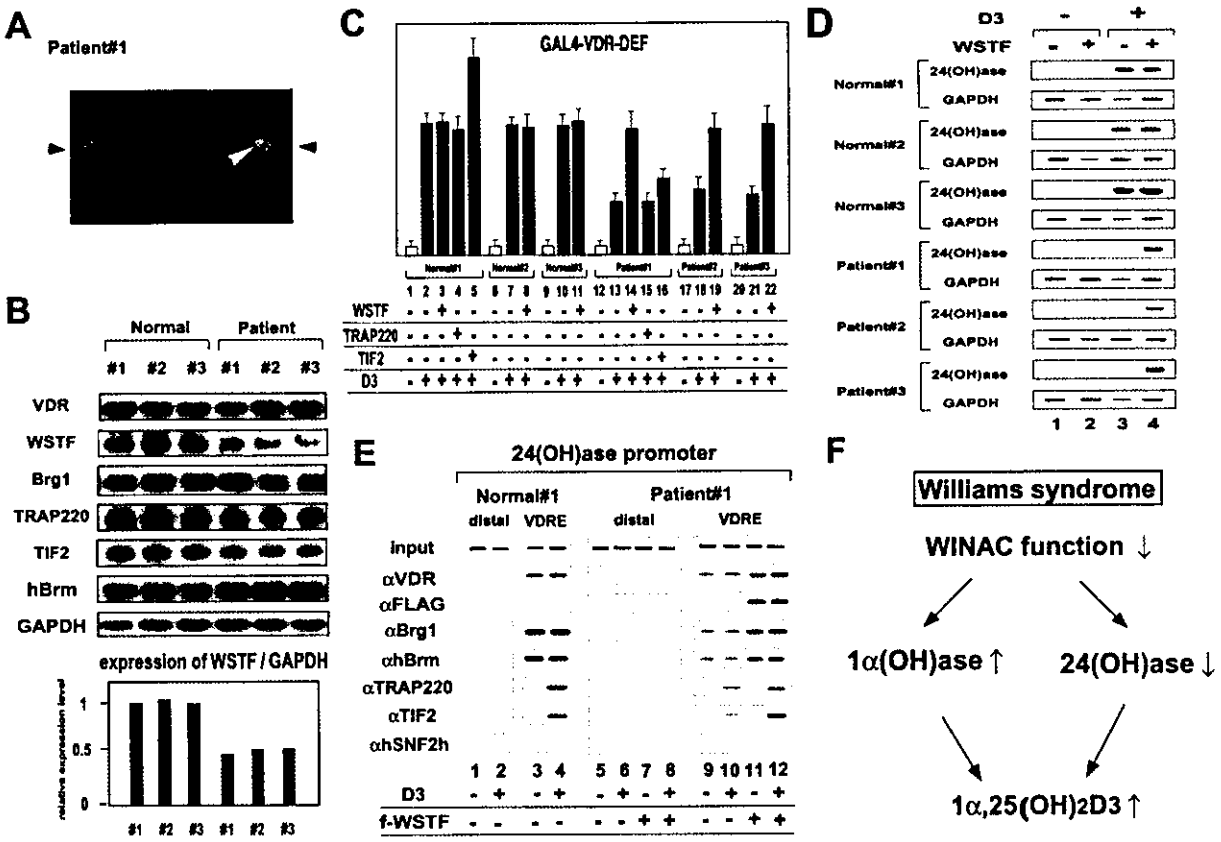

Figure 6. Impaired VDR Function In the Fibroblasts of Williams Syndrome Patients Was Recovered by WSTF Overexpression

(A) Fluorescence in situ hybridization of WS patient 1, confirming a deletion of one copy of the WSTF gene. The black arrowhead indicates D7S427 gene locus and the white arrowhead for WSTF gene. D7S427 was used for a chromosome 7 marker and cosmid full-length WSTF for WSTF gene probe.

(B) Reduced WSTF expression levels in WS skin fibroblasts. The indicated genes were examined for expression by Northern blotting with GAPDH expression as an internal control (Yanagisawa et al., 2002). Densitometric analysis of the relative expression level of WSTF versus GAPDH is shown in the lower image.

(C) VDR transactivation functions were impaired in the skin fibroblasts of the WS patients. Fibroblasts from controls and patients were transfected with the expression vectors as described in Figure 5A and the receptor function was tested.

(D) WSTF overexpression recovered the impaired responsiveness to vitamin D during 24(OH)ase gene induction. Patient's skin fibroblasts were transfected with an adenovirus expressing FLAG-WSTF, and treated with 1α,25(OH)2D3 (10^{-9} M) for 12 hr. Total RNA was subjected to RT-PCR analysis of 24(OH)ase expression.

(E) Impaired promoter targeting of VDR, coregulators, and WINAC components in fibroblasts from WS patients was rescued by WSTF overexpression. ChIP assays of the patient skin fibroblasts were performed with adenovirus expressing FLAG-WSTF as described in Figure 5B.

(F) Hypothesis of the cause of hypercalcemia in Williams syndrome patients.

methods we could detect neither the PBAF complex nor its specific component (BAF180). Moreover, by our purification, no ISWI-based complex was detectable even in the glycerol gradient fractions containing complexes with expected molecular weights. These observations are also different from a report that WSTF forms a hISWI-based chromatin-remodeling complex (Bozhenok et al., 2002). Confirming that hISWI (hSNF2h) expression did not affect the VDR transactivation function (Figures 5A and 5B), the combination with ISWI-based complex components looks to deter WSTF from the VDR interaction.

Of note, WINAC harbors three components, which have not yet been found in the ATP-dependent chromatin-remodeling complexes. Two factors (CAF-1p150 and TopoIIβ are integrated in the complexes serving roles in DNA replication (Smith and Stillman, 1989; Varga-Weisz et al., 1997), while FACT p140 is involved in a complex that promotes chromatin-dependent transcriptional elongation with an ISWI-type complex (LeRoy et al., 1998). From the observed WSTF interactions with the other subunits in vitro (Figures 3A–3D), WSTF appears to serve as a core protein to form an SWI2/SNF2-based complex, generating a subclass of the ATP-dependent chromatin-remodeling complex with DNA replication-related factors. Taken together, WSTF may serve as a dual platform protein capable of forming both SWI/SNF- and ISWI-type chromatin-remodeling complexes by distinct subunit combinations, but only the SWI/SNF-type WINAC selectively assists VDR function through a physical interaction.

WINAC Is a Chromatin-Remodeling Complex

Specific and more efficient targeting of VDR through WINAC to the VDREs was supported from functional analyses of the purified WINAC in vitro. In this respect,

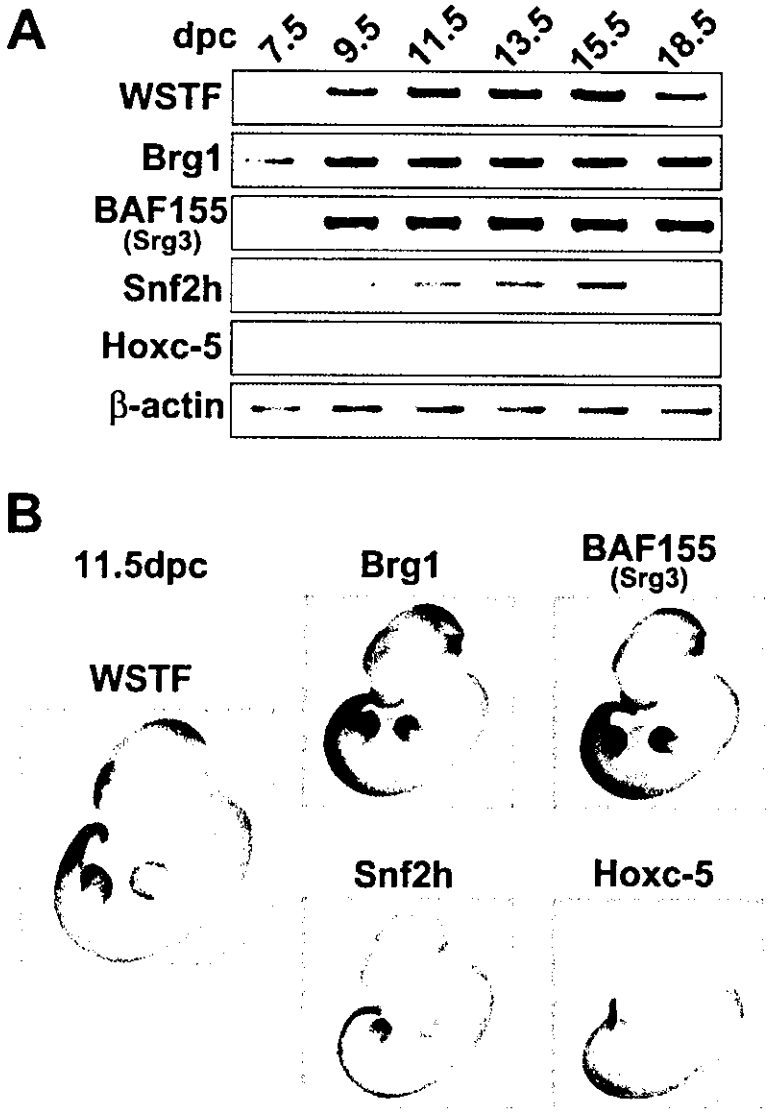

Figure 7. Spatiotemporal Expression Patterns of WSTF during Mouse Embryogenesis

(A) RT-PCR analysis of mouse WSTF, Brg1, BAF155 (Srg3), Snf2h, Hoxc-5, and β-actin gene expression. Embryos were dissected at the indicated times (7.5 dpc to 18.5 dpc). Samples were normalized by dilution to give equivalent signals for β-actin.

(B) Whole mount in situ hybridization analysis of mouse WSTF, Brg1, BAF155 (Srg3), Snf2h, and Hoxc-5 (negative control) expression at 11.5 dpc (Scale bar: 2 mm. Sense control probes were also hybridized and no signal was detected; data not shown).

WINAC subunit configuration is of interest to be clarified for defining the function of each component. A recent report has revealed that the chromatin-remodeling activity of the dISWI-based complex requires multiple Acf1 motifs to nonspecifically anchor DNA through its WAC motifs, and to directly interact with ISWI through the DDT domain (Fyodorov and Kadonaga, 2002). In addition to a core subunit role of WSTF, multiple functions as a pivotal factor to conduct the WINAC function could be further speculated from the conservation of several motifs that are shared with the other WAC family proteins, like hACF1 (Jones et al., 2000). Moreover, functions of the bromodomain and PHD finger motif in WSTF remain to be established in the promoter targeting and chromatin remodeling (Hassan et al., 2002; Schultz et al., 2002).

Promoter Targeting of VDR by WINAC and Cooperative WINAC Function with the Coregulator Complexes

Similar to the reported coactivator-like actions of the SWI2/SNF2 ATPases and BAF57 for the ligand-induced ERα transactivation (Chiba et al., 1994; DiRenzo et al., 2000; Belandia et al., 2002), overexpression of WSTF and the ATPase subunits as well could coactivate the ligand-induced VDR transactivation as either a GAL4 DBD chimeric protein or heterodimer with RXR (Figures 5A and 5C). VDR coactivation by the ligand-dependent NR coactivators (TIF2 and TRAP220) was abrogated by WSTF-RNAi expression (Figure 5A). However, neither such coactivator-like WSTF actions nor reduced coactivation by NR coactivators by the WSTF-RNAi expression was detected for ERα (Figure 5A) and the other receptors tested (data not shown), supporting the observed direct and selective interaction of WSTF with VDR among NRs (Figure 1D). Moreover, WSTF overexpression potentiated the ligand-induced transrepression of VDR on the 1α(OH)ase negative VDRE (Figure 5D), where an ablation of endogenous WSTF by RNAi expression led to a significant reduction in ligand-induced corepressor recruitment (lane 10 in Figure 5B). Thus, ligand-independent association of WINAC and VDR in the VDR target promoters appears to facilitate the local nucleosomal array

accessibility for ligand-dependent coregulators, following histone tail modifications by the recruited coregulator complexes (Hassan et al., 2002). It was recently reported that only when ligand is bound to ERα, all of the ERα p160/CBP HAT coactivator complex and human SWI/SNF-type complexes are targeted to the ER target promoters, although such ligand-induced occupancy of ERα and coregulator in the promoters appears in a cyclic fashion (Shang et al., 2000; Belandia et al., 2002). Such ligand-induced assembly of the SWI/SNF-type complexes with NRs through the p160/CBP complex might be a common mechanism for ligand-dependent targeting of NRs to the cognate promoters (Glass and Rosenfeld, 2000).

Unlike NRs such as ERα and AR (Belandia et al., 2002; Shang et al., 2002), VDR appears from ChIP analysis (Figure 5B) to be selectively targeted through WINAC to the promoters without ligand-induced activation of VDR function or following recruitment of coregulator complexes. WINAC targeting to the promoters appears not to require specific histone tail modifications by coregulators. Thus, it is likely that WINAC associating on promoters escort VDR for its recognition and specific binding to VDREs, through nucleosomal mobilization by WINAC, presumably cooperating with the other chromatin complexes (Lemon et al., 2001). Alternatively, once VDR happens to bind VDREs during nonspecific chromatin remodeling, WINAC might be acquired to VDR upon the promoters to engage in local nucleosome reorganization. The latter possibility coincides well with a recent report about a sequence-specific regulator, SATB1 (Yasui et al., 2002). As a result, the local chromatin structure near VDREs may transit into an active chromosomal state that appears competent for receipt of both the coactivator complexes and the corepressor complexes (Figures 5C and 5D) dependent on the VDRE sequences and the tertiary positions of DNA-bound VDR. This is not consistent with recent observations that the chromatin-remodeling complexes are recruited only after acetylation/deacetylation of histone tails by the coregulatory complexes (Hassan et al., 2002). However, the orders of the complex targetings are supposed to be dependent on the regulator type and the promoter context (Lomvardas and Thanos, 2002; Soutoglou and Talianidis, 2002).

Williams Syndrome Is a Chromatin-Remodeling Factor Disease?

We found that the ligand-induced transactivation function of VDR is impaired in the skin fibroblast cells of all three tested patients, in whom the regions covering the WSTF gene locus at the chromosome 7q11.23 are heterozygously deleted. Such impaired VDR function should not lead to severe defects in vitamin D actions in adults, since the adult VDR heterozygote mice ($VDR^{+/-}$) and the heterozygous carrier patients of the hereditary vitamin D-dependent type II rickets caused by VDR inactivation exhibited no overt abnormality in calcium and vitamin D metabolism, though VDR is a major regulator in those metabolisms (Yoshizawa et al., 1997). However, during growth, the mineral intakes must be greater than their excretions through the actions of calciotropic hormones, including vitamin D. It is tempting to speculate that the significantly reduced WINAC levels in WS patients transiently cause impaired function in VDR and other unidentified factors, leading to the transient appearance of infantile aberrant vitamin D metabolism and consequently, hypercalcemia (Taylor et al., 1982; Garabedian et al., 1985). These findings together suggest that a normal WSTF dose in the cells is necessary to support normal activities of VDR and presumably of some other regulators.

WSTF expression patterns during mouse embryogenesis overlap with those of the common components of WINAC (Bultman et al., 2000; Kim et al., 2001), but appear more limited. In contrast, the more restricted expression pattern was detected in mouse ISWI (Snf2h) (Lazzaro and Picketts, 2001) (Figure 7B). It is therefore possible to suggest that specific roles of WINAC among the other chromatin-remodeling complexes exert in a more spatiotemporal manner and support organogenesis of several selected tissues during embryogenesis through chromatin remodeling for, at least, transcription and DNA replication. Therefore, the WS patients may suffer a wide spectrum of disorders in certain organs. Thus, this study suggests that the Williams syndrome disorders are caused, at least in part, by WINAC dysfunction as a chromatin-remodeling disease.

Experimental Procedures

Plasmids and Antibodies

Chimeric GST proteins of GAL4 DBD (1–147 aa) fused with Rat VDR-DEF and WSTF deletion mutants were expressed in pGEX-2TK (Pharmacia Biotech). The promoter region of 1α,25-dihydroxyvitamin D3 24-hydroxylase (−367 to 0) and 25-hydroxyvitamin D3 1α-hydroxylase (−889 to −30) were inserted into the pGL3 vector (Promega) driven by a thymidine kinase (tk) promoter (Chen and DeLuca, 1995; Murayama et al., 1998; Yanagisawa et al., 2002). Rabbit polyclonal antipeptide antiserum was prepared by Sawady technology against KLQSEDSAKTEEVDEEKK, which is near the human WSTF C terminus.

Purification and Separation of VDR-Associated Complexes

For WINAC purification, the nuclear extracts of the MCF7 stable transformant were prepared by the same method as HeLa nuclear extracts (Rachez et al., 1998; Kitagawa et al., 2002; Yanagisawa et al., 2002). Then, they were bound to the GST column [GST], and 1α,25(OH)2D3-unbound GST-VDR column [GST-VDR(D3-)]. The complexes bound to the ligand-unbound VDR were eluted with 15 mM reduced glutathione in elution buffer (50 mM Tris-HCl [pH 8.3], 150 mM KCl, 0.5 mM EDTA, 0.5 mM PMSF, 5 mM NaF, 0.08% NP-40, 0.5 mg/ml BSA, and 10% glycerol). Next, they were layered on top of a 4.5 ml linear 100%–40% glycerol gradient in the GST binding buffer and centrifuged for 16 hr at 4°C at 40,000 rpm in a SW40 rotor (Beckman). Protein standards were ovalbumin (44 kDa), β-globulin (158 kDa), and thyroglobulin (667 kDa). Finally, the fractions containing WSTF and VDR were collected and loaded onto a 2.5–5 ml anti-FLAG M2 resin column (Sigma). After washing with binding buffer, the bound proteins were eluted by incubation for 60 min with 10–15 ml of the FLAG peptide (0.2 mg/ml) (Sigma) in binding buffer.

In Vitro Chromatin Reconstitution and Disruption Assay

Chromatin reconstitution and disruption reactions were performed essentially as previously described (Ito et al., 2000) using supercoiled plasmid DNA. A standard reaction contained plasmid (0.4 μg), purified core histones from *Drosophila* embryos (0.33 μg), purified recombinant dNAP1 (2.8 μg) [dNAP1], purified recombinant ACF (40 ng) [dACF], purified WINAC (100 ng) [WINAC], ATP (3 mM), and the ATP-regenerating system (30 mM phosphocreatine and 1mg/ml creatine phosphokinase). For the chromatin-disruption assay,

chromatin was reconstituted with DNA, pGIE0 (containing the GAL4 binding site) and purified histones by salt dialysis, and GST-GAL4 fusion proteins [e.g., GAL-VDR] mediated disruption of nucleosome arrays was analyzed by micrococcal nuclease digestion-Southern blot analysis.

In Vitro Transcription Assay

The purified proteins were purified as described previously (Ito et al., 2000). An in vitro transcription reactions and primer extension analysis was performed with pGI0 as an internal control, as previously described (Ito et al., 1997). Chromatin was reconstituted with DNA, pGIE0 (0.2 μg), and purified histones (0.24 μg) by salt dialysis and indicated purified GST-GAL4 fusion proteins (50 nM each final concentration), purified WINAC (50 ng) [WINAC] and p300 (40 nM) [p300] were added before the transcription reactions. After primer extension reactions, ^{32}P-labeled DNA was extracted by phenol-chroroform, precipitated by ethanol, analyzed on 8% acrylamide 8.3 M urea gels, and visualized by autoradiography.

In Vitro Replication Assay

An in vitro replication assay was performed as previously described (Ohba et al., 1996). Purified WINAC [WINAC], purified recombinant *Drosophila* NAP-1 [dNAP1], or *Drosophila* CAF-1[dCAF1] was added before initiating the DNA replication reactions. The products were extracted and subjected to electrophoresis in a 1.5% agarose gel (1 × TBE) and visualized by autoradiography.

Cell Cycle Analysis Using RNAi and DNA Quantity Analysis

For immunoprecipitation during the double-thymidine treatment, about 80% of the confluent cells of FLAG-WSTF stable transformants were treated with thymidine (2.5 mM). After 24 hr, the cells were washed and cultured in normal medium for 10 hr (first release), then were treated with hydroxyurea (1 mM), and cultured for 16 hr (Fujita et al., 1996). Finally, the cells were washed and cultured in normal conditions (final release), then immunoprecipitated with anti-FLAG M2-resin. For the analysis of the DNA histogram, the FACS analysis was done using FACS Calibur (BD PharMingen) and CellQuest (BD PharMingen) (Fujita et al., 1996).

RNAi Experiments

The two short RNAs were transfected after they were annealed. The sequence of the indicated RNAi is as follows: WSTF-RNAi (5′-GAGUAUGAAGCCCGCUUGGTT-3′ and 5′-CCAAGCGGGCUUCAUAC-UCTT-3′); Brg1-RNAi (5′-CUCCUCGGCCAGGUCCUUCTT-3′ and 5′-GAA-GGACCUGGCCGAGGAGTT-3′); Brm-RNAi (5′-UUCUUGGGCCUAGUC-CAGGTT-3′ and 5′-CCUGGACUAGGCCCAAGAATT-3′); CAF-1 p150-RNAi (5′-UCUUGUCCCAAA-GGGGAAATT-3′ and 5′-UUUCCCCUUUGG-GACAAGATT-3′); and control-RNAi (5′-CAGUAAGUAGCCGGGAUGGTT-3′ and 5′-CCAUCCCGGCUACUUACUGTT-3′).

ChIP Assay

Preparation of soluble chromatin for PCR amplification was performed as previously reported (Shang et al., 2000; Yanagisawa et al., 2002). The primer pairs for 24(OH)ase were 5′-GGGAGGCGCGTTCGAA-3′ and 5′-TCCTATGCCCAG-GGAC-3′ (pVDRE) and 5′-CCTCCTTTGCACAAGG-TAGT-3′ and 5′-AATGCACGTAAAGCGGCA-AC-3′ (distal); the primers for 1a(OH)ase were 5′-ATTCCCATGTCTGGAAGGAG-3′ and 5′-CAGTGAGC-CCAGCCCCTTTA-3′ (nVDRE) and 5′-AAGCTTGTCTCAACCTCCTG-3′ and 5′-GTTCAGAGATTGTCTGTGGG-3′ (distal).

Acknowledgments

We thank Dr. Michael Jones for kindly providing the partial WSTF cDNAs; Dr. H. Kato and Dr. H. Iba for Brg1 and hBrm plasmids; Dr. J. Kadonaga for dNAP-1; Dr. C. Wu for dACF; Dr. J.K. Tyler for dCAF-1; and Drs. G. Mizuguchi and L. Freedman for technical discussion. We also thank Dr. K. Yamane, H. Kawano, and A. Unno for the technical support; Dr. L. Tora for the critical discussion; and Miss H. Higuchi for preparation of the manuscript. This work was supported in part by a grant-in-aid for priority areas from the Ministry of Education, Science, Sports, and Culture of Japan (S.K.).

Received: December 30, 2002
Revised: May 16, 2003
Accepted: May 28, 2003
Published: June 26, 2003

References

Belandia, B., Orford, R.L., Hurst, H.C., and Parker, M.G. (2002). Targeting of SWI/SNF chromatin remodelling complexes to estrogen-responsive genes. EMBO J. *21*, 4094–4103.

Bozhenok, L., Wade, P.A., and Varga-Weisz, P. (2002). WSTF-ISWI chromatin remodeling complex targets heterochromatic replication foci. EMBO J. *21*, 2231–2241.

Bultman, S., Gebuhr, T., Yee, D., La Mantia, C., Nicholson, J., Gilliam, A., Randazzo, F., Metzger, D., Chambon, P., Crabtree, G., and Magnuson, T. (2000). A Brg1 null mutation in the mouse reveals functional differences among mammalian SWI/SNF complexes. Mol. Cell *6*, 1287–1295.

Chen, K.S., and DeLuca, H.F. (1995). Cloning of the human 1 alpha,25-dihydroxyvitamin D-3 24-hydroxylase gene promoter and identification of two vitamin D-responsive elements. Biochim. Biophys. Acta *1263*, 1–9.

Chiba, H., Muramatsu, M., Nomoto, A., and Kato, H. (1994). Two human homologues of Saccharomyces cerevisiae SWI2/SNF2 and Drosophila brahma are transcriptional coactivators cooperating with the estrogen receptor and the retinoic acid receptor. Nucleic Acids Res. *22*, 1815–1820.

DiRenzo, J., Shang, Y., Phelan, M., Sif, S., Myers, M., Kingston, R., and Brown, M. (2000). BRG-1 is recruited to estrogen-responsive promoters and cooperates with factors involved in histone acetylation. Mol. Cell. Biol. *20*, 7541–7549.

Elbashir, S.M., Harborth, J., Lendeckel, W., Yalcin, A., Weber, K., and Tuschl, T. (2001). Duplexes of 21-nucleotide RNAs mediate RNA interference in cultured mammalian cells. Nature *411*, 494–498.

Emerson, B.M. (2002). Specificity of gene regulation. Cell *109*, 267–270.

Fujita, M., Kiyono, T., Hayashi, Y., and Ishibashi, M. (1996). hCDC47, a human member of the MCM family. Dissociation of the nucleus-bound form during S phase. J. Biol. Chem. *271*, 4349–4354.

Fyodorov, D.V., and Kadonaga, J.T. (2001). The many faces of chromatin remodeling: SWItching beyond transcription. Cell *106*, 523–525.

Fyodorov, D.V., and Kadonaga, J.T. (2002). Binding of Acf1 to DNA involves a WAC motif and is important for ACF-mediated chromatin assembly. Mol. Cell. Biol. *22*, 6344–6353.

Garabedian, M., Jacqz, E., Guillozo, H., Grimberg, R., Guillot, M., Gagnadoux, M.F., Broyer, M., Lenoir, G., and Balsan, S. (1985). Elevated plasma 1,25-dihydroxyvitamin D concentrations in infants with hypercalcemia and an elfin facies. N. Engl. J. Med. *312*, 948–952.

Glass, C.K., and Rosenfeld, M.G. (2000). The coregulator exchange in transcriptional functions of nuclear receptors. Genes Dev. *14*, 121–141.

Gu, W., Malik, S., Ito, M., Yuan, C.X., Fondell, J.D., Zhang, X., Martinez, E., Qin, J., and Roeder, R.G. (1999). A novel human SRB/MED-containing cofactor complex, SMCC, involved in transcription regulation. Mol. Cell *3*, 97–108.

Hassan, A.H., Prochasson, P., Neely, K.E., Galasinski, S.C., Chandy, M., Carrozza, M.J., and Workman, J.L. (2002). Function and selectivity of bromodomains in anchoring chromatin-modifying complexes to promoter nucleosomes. Cell *111*, 369–379.

Hoogenraad, C.C., Koekkoek, B., Akhmanova, A., Krugers, H., Dortland, B., Miedema, M., van Alphen, A., Kistler, W.M., Jaegle, M., Koutsourakis, M., et al. (2002). Targeted mutation of Cyln2 in the Williams syndrome critical region links CLIP-115 haploinsufficiency to neurodevelopmental abnormalities in mice. Nat. Genet. *32*, 116–127.

Ito, T., Bulger, M., Pazin, M.J., Kobayashi, R., and Kadonaga, J.T. (1997). ACF, an ISWI-containing and ATP-utilizing chromatin assembly and remodeling factor. Cell *90*, 145–155.

Ito, T., Ikehara, T., Nakagawa, T., Kraus, W.L., and Muramatsu, M. (2000). p300-mediated acetylation facilitates the transfer of histone H2A–H2B dimers from nucleosomes to a histone chaperone. Genes Dev. *14*, 1899–1907.

Jones, M.H., Hamana, N., Nezu, J., and Shimane, M. (2000). A novel family of bromodomain genes. Genomics *63*, 40–45.

Kamei, Y., Xu, L., Heinzel, T., Torchia, J., Kurokawa, R., Gloss, B., Lin, S.C., Heyman, R.A., Rose, D.W., Glass, C.K., and Rosenfeld, M.G. (1996). A CBP integrator complex mediates transcriptional activation and AP-1 inhibition by nuclear receptors. Cell *85*, 403–414.

Kim, J.K., Huh, S.O., Choi, H., Lee, K.S., Shin, D., Lee, C., Nam, J.S., Kim, H., Chung, H., Lee, H.W., et al. (2001). Srg3, a mouse homolog of yeast SWI3, is essential for early embryogenesis and involved in brain development. Mol. Cell. Biol. *21*, 7787–7795.

Kitagawa, H., Yanagisawa, J., Fuse, H., Ogawa, S., Yogiashi, Y., Okuno, A., Nagasawa, H., Nakajima, T., Matsumoto, T., and Kato, S. (2002). Ligand-selective potentiation of rat mineralocorticoid receptor activation function 1 by a CBP-containing histone acetyltransferase complex. Mol. Cell. Biol. *22*, 3698–3706.

Lazzaro, M.A., and Picketts, D.J. (2001). Cloning and characterization of the murine imitation switch (ISWI) genes: differential expression patterns suggest distinct developmental roles for Snf2h and Snf2l. J. Neurochem. *77*, 1145–1156.

Lemon, B., Inouye, C., King, D.S., and Tjian, R. (2001). Selectivity of chromatin-remodelling cofactors for ligand-activated transcription. Nature *414*, 924–928.

LeRoy, G., Orphanides, G., Lane, W.S., and Reinberg, D. (1998). Requirement of RSF and FACT for transcription of chromatin templates in vitro. Science *282*, 1900–1904.

Lomvardas, S., and Thanos, D. (2002). Modifying gene expression programs by altering core promoter chromatin architecture. Cell *110*, 261–271.

Loyola, A., LeRoy, G., Wang, Y.H., and Reinberg, D. (2001). Reconstitution of recombinant chromatin establishes a requirement for histone-tail modifications during chromatin assembly and transcription. Genes Dev. *15*, 2837–2851.

Lu, X., Meng, X., Morris, C.A., and Keating, M.T. (1998). A novel human gene, WSTF, is deleted in Williams syndrome. Genomics *54*, 241–249.

Mangelsdorf, D.J., Thummel, C., Beato, M., Herrlich, P., Schutz, G., Umesono, K., Blumberg, B., Kastner, P., Mark, M., Chambon, P., et al. (1995). The nuclear receptor superfamily: the second decade. Cell *83*, 835–839.

Murayama, A., Takeyama, K., Kitanaka, S., Kodera, Y., Hosoya, T., and Kato, S. (1998). The promoter of the human 25-hydroxyvitamin D3 1 alpha-hydroxylase gene confers positive and negative responsiveness to PTH, calcitonin, and 1 alpha,25(OH)2D3. Biochem. Biophys. Res. Commun. *249*, 11–16.

Narlikar, G.J., Fan, H.Y., and Kingston, R.E. (2002). Cooperation between complexes that regulate chromatin structure and transcription. Cell *108*, 475–487.

Ohba, R., Matsumoto, K., and Ishimi, Y. (1996). Induction of DNA replication by transcription in the region upstream of the human c-myc gene in a model replication system. Mol. Cell. Biol. *16*, 5754–5763.

Onate, S.A., Tsai, S.Y., Tsai, M.J., and O'Malley, B.W. (1995). Sequence and characterization of a coactivator for the steroid hormone receptor superfamily. Science *270*, 1354–1357.

Peoples, R.J., Cisco, M.J., Kaplan, P., and Francke, U. (1998). Identification of the WBSCR9 gene, encoding a novel transcriptional regulator, in the Williams-Beuren syndrome deletion at 7q11.23. Cytogenet. Cell Genet. *82*, 238–246.

Poot, R.A., Dellaire, G., Hulsmann, B.B., Grimaldi, M.A., Corona, D.F., Becker, P.B., Bickmore, W.A., and Varga-Weisz, P.D. (2000). HuCHRAC, a human ISWI chromatin remodelling complex contains hACF1 and two novel histone-fold proteins. EMBO J. *19*, 3377–3387.

Rachez, C., Suldan, Z., Ward, J., Chang, C.P., Burakov, D., Erdjument-Bromage, H., Tempst, P., and Freedman, L.P. (1998). A novel protein complex that interacts with the vitamin D3 receptor in a ligand-dependent manner and enhances VDR transactivation in a cell-free system. Genes Dev. *12*, 1787–1800.

Schultz, D.C., Ayyanathan, K., Negorev, D., Maul, G.G., and Rauscher, F.J., 3rd. (2002). SETDB1: a novel KAP-1-associated histone H3, lysine 9-specific methyltransferase that contributes to HP1-mediated silencing of euchromatic genes by KRAB zinc-finger proteins. Genes Dev. *16*, 919–932.

Sekine, K., Ohuchi, H., Fujiwara, M., Yamasaki, M., Yoshizawa, T., Sato, T., Yagishita, N., Matsui, D., Koga, Y., Itoh, N., and Kato, S. (1999). Fgf10 is essential for limb and lung formation. Nat. Genet. *21*, 138–141.

Shang, Y., Hu, X., DiRenzo, J., Lazar, M.A., and Brown, M. (2000). Cofactor dynamics and sufficiency in estrogen receptor-regulated transcription. Cell *103*, 843–852.

Shang, Y., Myers, M., and Brown, M. (2002). Formation of the androgen receptor transcription complex. Mol. Cell *9*, 601–610.

Smith, S., and Stillman, B. (1989). Purification and characterization of CAF-I, a human cell factor required for chromatin assembly during DNA replication in vitro. Cell *58*, 15–25.

Soutoglou, E., and Talianidis, I. (2002). Coordination of PIC assembly and chromatin remodeling during differentiation-induced gene activation. Science *295*, 1901–1904.

Taylor, A.B., Stern, P.H., and Bell, N.H. (1982). Abnormal regulation of circulating 25-hydroxyvitamin D in the Williams syndrome. N. Engl. J. Med. *306*, 972–975.

Varga-Weisz, P.D., Wilm, M., Bonte, E., Dumas, K., Mann, M., and Becker, P.B. (1997). Chromatin-remodelling factor CHRAC contains the ATPases ISWI and topoisomerase II. Nature *388*, 598–602.

Yanagisawa, J., Kitagawa, H., Yanagida, M., Wada, O., Ogawa, S., Nakagomi, M., Oishi, H., Yamamoto, Y., Nagasawa, H., McMahon, S.B., et al. (2002). Nuclear receptor function requires a TFTC-type histone acetyl transferase complex. Mol. Cell *9*, 553–562.

Yasui, D., Miyano, M., Cai, S., Varga-Weisz, P., and Kohwi-Shigematsu, T. (2002). SATB1 targets chromatin remodelling to regulate genes over long distances. Nature *419*, 641–645.

Yoshizawa, T., Handa, Y., Uematsu, Y., Takeda, S., Sekine, K., Yoshihara, Y., Kawakami, T., Arioka, K., Sato, H., Uchiyama, Y., et al. (1997). Mice lacking the vitamin D receptor exhibit impaired bone formation, uterine hypoplasia and growth retardation after weaning. Nat. Genet. *16*, 391–396.

The EMBO Journal (2004) 23, 4813–4823 | © 2004 European Molecular Biology Organization | All Rights Reserved 0261-4189/04
www.embojournal.org

THE EMBO JOURNAL

Ligand-dependent switching of ubiquitin–proteasome pathways for estrogen receptor

Yukiyo Tateishi[1,6], Yoh-ichi Kawabe[1,6], Tomoki Chiba[2], Shigeo Murata[2], Ken Ichikawa[1], Akiko Murayama[1], Keiji Tanaka[2], Tadashi Baba[1], Shigeaki Kato[3,4] and Junn Yanagisawa[1,5,*]

[1]Graduate School of Life and Environmental Sciences, University of Tsukuba, Tsukuba Science City, Ibaraki, Japan, [2]The Tokyo Metropolitan Institute of Medical Science, Bunkyo-ku, Tokyo, Japan, [3]Institute of Molecular and Cellular Biosciences, University of Tokyo, Bunkyo-ku, Tokyo, Japan, [4]SORST, Japan Science and Technology, Kawaguchi, Saitama, Japan and [5]Ankhs Inc., Tsukuba-city, Ibaraki, Japan

Recent evidence indicates that the transactivation of estrogen receptor α (ERα) requires estrogen-dependent receptor ubiquitination and degradation. Here we show that estrogen-unbound (unliganded) ERα is also ubiquitinated and degraded through a ubiquitin–proteasome pathway. To investigate this ubiquitin–proteasome pathway, we purified the ubiquitin ligase complex for unliganded ERα and identified a protein complex containing the carboxyl terminus of Hsc70-interacting protein (CHIP). CHIP preferentially bound to misfolded ERα and ubiquitinated it to induce degradation. Ligand binding to the receptor induced the dissociation of CHIP from ERα. In CHIP−/− cells, the degradation of unliganded ERα was abrogated; however, estrogen-induced degradation was observed to the same extent as in CHIP+/+ cells. Our findings suggest that ERα is regulated by two independent ubiquitin–proteasome pathways, which are switched by ligand binding to ERα. One pathway is necessary for the transactivation of the receptor and the other is involved in the quality control of the receptor.

The EMBO Journal (2004) **23**, 4813–4823. doi:10.1038/sj.emboj.7600472; Published online 11 November 2004
Subject Categories: chromatin & transcription; proteins
Keywords: estrogen receptor; nuclear receptors transcription; ubiquitination

Introduction

The effects of estrogen are mediated through the estrogen receptors ERα and ERβ, which function as ligand-induced transcriptional factors and belong to the nuclear receptor superfamily (Beato *et al*, 1995; Mangelsdorf *et al*, 1995; Chambon, 1996; McKenna and O'Malley, 2002). Estrogen binding to its receptor induces the ligand-binding domain (LBD) to undergo a characteristic conformational change, whereupon the receptor dimerizes, binds to DNA and subsequently stimulates the gene expression. ERα is stimulated by two distinct activation regions, activation function-1 (AF-1) and AF-2, which are located in the C-terminal LBD and exert ligand-dependent transcriptional activity. Cellular response to estrogen is tightly controlled, and a large number of ERα-interacting proteins have been described as coactivators or corepressors that modify ERα transcriptional activity (Shang *et al*, 2000; Yanagisawa *et al*, 2002; Metivier *et al*, 2003).

Crystal-structural analysis of ERα and other nuclear receptors has revealed the presence of 12 conserved helices in their LBD (Shiau *et al*, 1998). The LBD forms a structure described as a sandwich of 12 α-helices (Helices 1–12) with a central hydrophobic ligand-binding pocket. Helix 12, the most C-terminal of these helices, has been identified as the critical core (AD core) of the AF-2 function of the receptor and plays an important role in coactivator binding to the ligand-bound receptor. In the presence of the ligand, the hinge region between Helices 11 and 12 moves closer to Helices 3 and 5, and Helix 12 is positioned over the ligand-binding pocket formed by Helices 3–5. The repositioned Helix 12 forms a hydrophobic groove with Helices 3 and 5. This hydrophobic groove is known to be important for the interaction with LXXLL motifs found in coactivator molecules (Heery *et al*, 1997).

The activation of nuclear receptors appears to be coupled with the degradation of these proteins by the ubiquitin–proteasome pathway (Boudjelal *et al*, 2000; Dace *et al*, 2000; Blanquart *et al*, 2002). Several recent studies have focused on the involvement of the ubiquitin–proteasome pathway in the estrogen-dependent degradation of ERα, which can be blocked with specific inhibitors of proteasome function, such as MG132 and lactacystin. It has also been reported that the 26S proteasome is essential for estrogen-dependent ERα transcription activity (Nawaz *et al*, 1999a; Lonard *et al*, 2000; Reid *et al*, 2003). Furthermore, several components of the ubiquitin–proteasome pathway have been identified as nuclear receptor-interacting proteins, including SUG1/TRIP1 (Lee *et al*, 1995), RSP5/RPF1 (Imhof and McDonnell, 1996), E6-AP (Nawaz *et al*, 1999b) and UBC9 (Poukka *et al*, 1999). These observations suggest that the ubiquitin–proteasome pathway may play an important role in regulating nuclear receptor levels and restricting the duration and magnitude of receptor activity in response to ligands. Nonetheless, mechanisms governing ERα protein levels remain poorly understood.

Here we show that, in the absence of estrogen, ERα is also ubiquitinated and degraded via a ubiquitin–proteasome pathway. The observation that estrogen-dependent ubiquitination of the receptor required the AD core region within the ERαLBD, whereas the ubiquitination of the unliganded receptor did not, raised the possibility that the ubiquitin ligase for unliganded ERα might differ from the ligase involved in estrogen-dependent ubiquitination. Therefore, we purified

*Corresponding author. Graduate School of Life and Environmental Sciences, University of Tsukuba, 1-1-1 Tenno-dai, Tsukuba Science City, Ibaraki 305-8572, Japan. Tel.: +81 29 853 6632; Fax: +81 29 853 4605; E-mail: junny@agbi.tsukuba.ac.jp
[6]These authors contributed equally to this work

Received: 21 June 2004; accepted: 12 October 2004; published online: 11 November 2004

the ubiquitin-ligase complex for unliganded ERα and identified a chaperone complex containing the carboxyl terminus of Hsc70-interacting protein (CHIP) (Ballinger *et al*, 1999; Dai *et al*, 2003). CHIP selectively bound to and ubiquitinated misfolded ERα and stimulated the degradation of these receptors. This model was further supported by an experiment using CHIP-deficient mouse (CHIP−/−) embryonic fibroblast cells. The unliganded ERα was degraded in CHIP+/+ cells but not in CHIP−/− cells under thermally stressed conditions. In contrast, estrogen-dependent degradation was observed in both CHIP+/+ and CHIP−/− cells, supporting the idea that the inactive and active forms of the receptor are regulated by two independent ubiquitin–proteasome pathways. Our findings shed light on the ubiquitin–proteasome network regulating nuclear receptors.

Results

Unliganded ERα is degraded through a ubiquitin–proteasome pathway

As shown in Figure 1A, addition of estrogen to MCF-7 cells reduced the level of ERα protein. The reduction of ERα was inhibited by the proteasome inhibitors MG132 or lactacystin. In the absence of estrogen, MG132 or lactacystin treatment also resulted in ERα accumulation (Figure 1A, lanes 3 and 5), suggesting that not only estrogen-bound ERα but also unliganded ERα is degraded through proteasomes. In ubiquitination assay, ERα was ubiquitinated in both the presence and absence of estrogen (Figure 1B, lanes 3 and 4), indicating that this process is mediated through ubiquitin–proteasome pathways.

We next determined whether the degradation of unliganded and liganded ERα is regulated by the same ubiquitin–proteasome pathway. It has been reported that truncated ERα, ERαΔAD, which does not have an AD core domain, does not exhibit estrogen-dependent degradation (Lonard *et al*, 2000). Thus, we examined the ubiquitination and degradation of ERαΔAD. ERα and ERαΔAD were transfected into 293 cells and the ERα protein level was examined by Western blot analysis. While the ERα degradation was observed regardless of estrogen treatment, ERαΔAD was stabilized by ligand binding, as it accumulates in response to estrogen. MG132 treatment increases the levels of ERαΔAD in the absence of the ligand but does not affect its estrogen-induced accumulation (Figure 1C). We next tested whether ERαΔAD turnover is

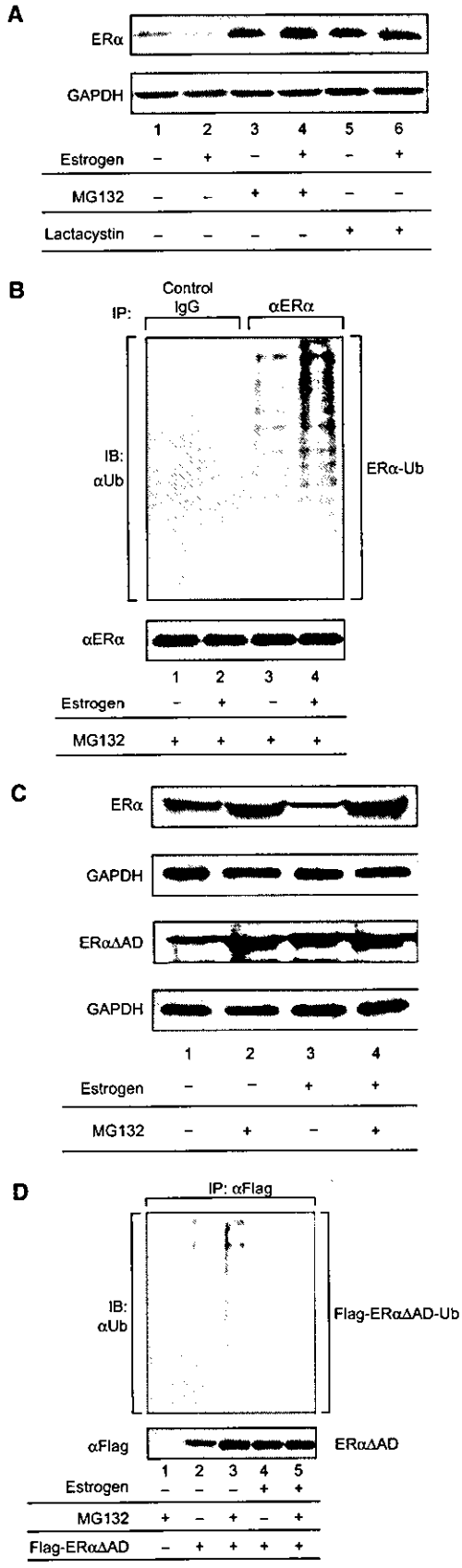

Figure 1 Unliganded ERα was degraded through a ubiquitin–proteasome pathway. (**A**) ERα was degraded in the absence of estrogen. The MCF-7 cells were cultured in the presence or absence of estrogen (10^{-8} M), or the proteasome inhibitor MG132 or lactacystin (10^{-6} M). ERα level was analyzed by Western blotting using anti-ERα monoclonal antibody. (**B**) ERα was ubiquitinated in the absence of estrogen. MCF-7 cells were cultured in the presence or absence of estrogen (10^{-8} M) or MG132 (10^{-6} M). ERα was immunoprecipitated using anti-ERα antibody. The ubiquitination status of ERα was analyzed by Western blotting using anti-ubiquitin antibody. (**C**) ERαΔAD was selectively degraded in the absence of estrogen. 293 cells were transfected with either ERα or ERαΔAD (500 ng). At 24 h post-transfection, the cells were cultured in the presence or absence of estrogen (10^{-8} M) or MG132 (10^{-6} M). ERα or ERαΔAD protein levels were analyzed by Western blotting using anti-ERα antibody. (**D**) ERαΔAD was ubiquitinated in the absence of estrogen. Flag-tagged ERαΔAD (500 ng) was transfected into 293 cells in the presence or absence of estrogen (10^{-8} M) or MG132 (10^{-6} M). Flag-tagged ERαΔAD was immunoprecipitated using anti-Flag M2 antibody. The ubiquitination status of ERαΔAD was analyzed by Western blotting using anti-ubiquitin antibody.

mediated through ubiquitination. In the absence of MG132, we detected almost no or little ubiquitination of ERαΔAD in the presence and absence of estrogen (Figure 1D, lanes 2 and 4). However, in the presence of MG132, we observed smeary bands of ubiquitin-conjugated ERαΔAD products in the absence of estrogen (Figure 1D, lane 3). These results indicate that while ERαΔAD shows no ligand-dependent ubiquitination, unliganded ERαΔAD is still degraded through ubiquitin–proteasome pathways. According to these results, there are possibly two independent ubiquitination pathways for ERα.

Unliganded ERα associates with a protein complex containing CHIP

We then investigated the region responsible for the degradation of unliganded ERα. The protein level of truncated ERα was examined by Western blotting in the presence or absence of estrogen. As shown in Figure 2A, all of the deletion mutants containing the E domain accumulated with estrogen treatment. MG132 treatment increased the levels of these mutants, indicating that they were degraded through proteasome (Figure 2A, lower panel). These results suggest that the region responsible for the degradation of unliganded ERα is located within ERαLBD. From these results, we speculated that an E3 ubiquitin ligase specifically binds and conjugates ubiquitin to the unliganded ERαLBD. We therefore attempted to identify the putative ubiquitin ligase for unliganded ERα. A HeLa cell extract-derived fraction was incubated with glutathione-*S*-transferase (GST)-fused ERαLBD in the presence or absence of estrogen. Proteins that interacted with ERαLBD were separated by SDS–polyacrylamide gel electrophoresis (SDS–PAGE) and silver stained (Figure 2B). To identify the proteins that selectively bound to unliganded ERαLBD, we performed peptide mass fingerprinting, and revealed that the 35 kDa protein eluted from the unliganded ERαLBD column consisted of CHIP (Figure 2B). The result obtained from peptide mass fingerprinting was confirmed by Western blotting using a specific antibody against CHIP (Figure 2B, lower panel).

CHIP is known to possess E3 ubiquitin-ligase activity mediated by its carboxy-terminal U-box domain and has the ability to bind to chaperones Hsp/Hsc70 by means of its tetratricopeptide repeat (TPR) domain (Scheufler *et al*, 2000; Connell *et al*, 2001; Imai *et al*, 2002). Mass spectrometric analysis also identified chaperone proteins Hsp/Hsc70 (Figure 2B), indicating that CHIP binds unliganded ERαLBD as a protein complex containing Hsp/Hsc70. Thus, we examined the interaction between ERα and CHIP/Hsp/Hsc70 complex using a co-immunoprecipitation method. As shown in Figure 2C, CHIP is selectively co-immunoprecipitated with

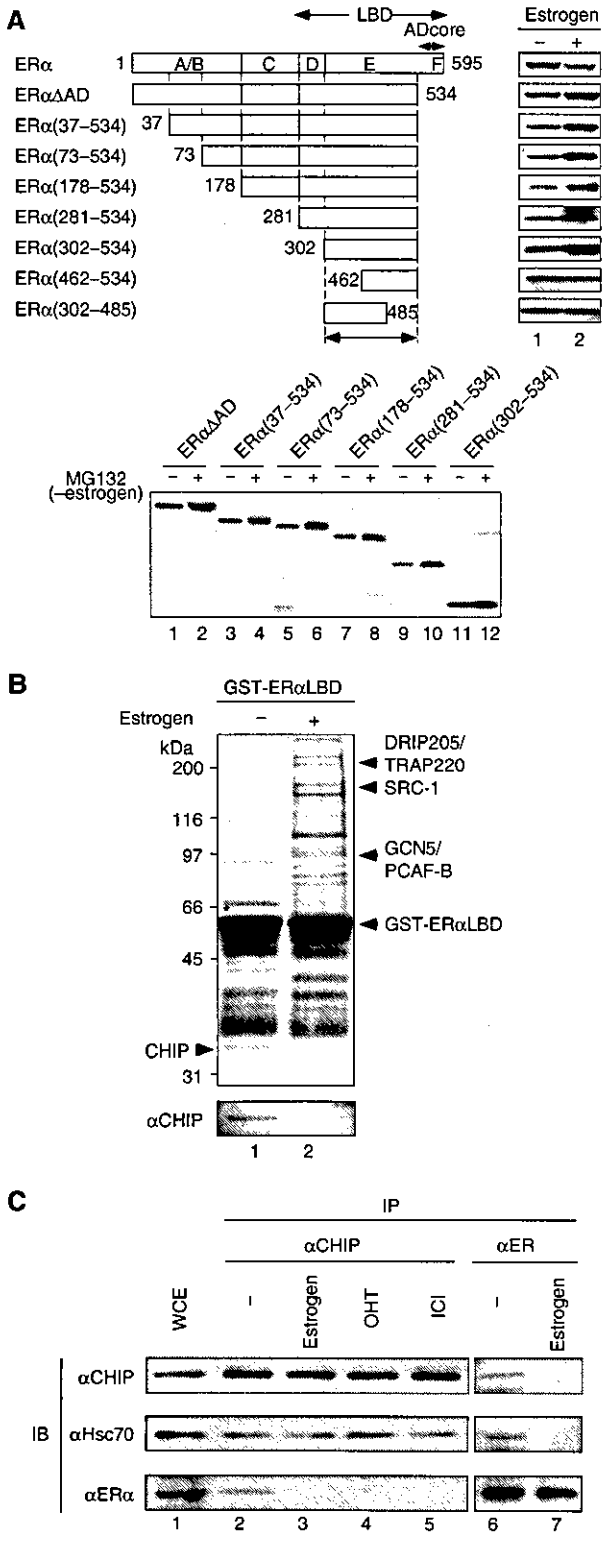

Figure 2 The unliganded ERα associated with a protein complex containing CHIP and Hsc/Hsp70. (**A**) The E region of ERα was sufficient for the degradation of unliganded ERα. Indicated Flag-tagged ERα deletion mutants (500 ng) were transfected into 293 cells. These cells were cultured in the presence or absence of estrogen (10^{-8} M) (upper panel) or MG132 (10^{-6} M) (lower panel). To evaluate the protein level of ERα mutants, Western blot analysis was performed using anti-Flag M2 antibody. (**B**) Purification and identification of ERαLBD-interacting proteins. Extracts prepared from HeLa S3 cells were incubated with immobilized GST-ERαLBD in the presence or absence of estrogen (10^{-6} M). ERα-interacting proteins were eluted from the GST-ERαLBD column by *N*-lauroyl sarkosin and subjected to SDS–PAGE followed by silver staining. The fractions eluted from unliganded GST-ERαLBD column (lane 1) and liganded GST-ERαLBD column (lane 2) are shown. Proteins eluted from both columns were examined by mass spectrometry. *Hsc70. (**C**) Interaction between unliganded ERα and CHIP *in vivo*. MCF-7 cells were lysed and subjected to immunoprecipitation using either anti-CHIP or anti-ERα antibody in the presence or absence of indicated ligands (estrogen (10^{-8} M); OHT: 4-hydroxytamoxifen (10^{-6} M); ICI: ICI182,780 (10^{-7} M)). The precipitates were Western blotted with antibodies for CHIP, ERα and Hsc70. MCF-7 whole-cell extract is shown in lane 1 (WCE).

unliganded ERα and Hsc70. Cell treatment with either 4-hydroxytamoxifen (OHT), a partial antagonist of ERα, or ICI182,780 (ICI), a pure antagonist of ERα, abrogated the binding between ERα and CHIP. CHIP was also detected in the immunoprecipitation performed with an anti-ERα antibody in the absence of ligands, confirming the interaction between ERα and CHIP *in vivo*. The same results were obtained in the human endometrial adenocarcinoma cell line Ishikawa (data not shown).

To better characterize and identify other components of the CHIP–Hsc70 complex, we generated HeLa cell lines stably expressing Flag-HA double-tagged CHIP. The protein complex containing CHIP was precipitated and separated by SDS–PAGE. Protein identification of the purified proteins by mass spectrometric analysis identified KIAA0678, Hsp90, Hsc70, Hsp70, Hsp40 and CHIP (Figure 3A). The protein components of the CHIP complex were confirmed by Western blotting using specific antibodies. Hsp90, Hsc70, Hsp70, Hsp40 and BAG-1 in the CHIP complex are shared with the chaperone components, whereas other chaperone components, Hip, Hop and p23, were undetectable by Western blot analysis (Figure 3B). To investigate whether this protein complex binds to unliganded ERα, Flag-tagged ERα expressed in 293 cells was immunoprecipitated using anti-Flag monoclonal antibody. As shown in Figure 3C, all of the components detected in the CHIP complex by Western blotting existed in the precipitant (Figure 3C, left panel). Next, to investigate whether this protein complex has the same composition in physiological conditions, ERα was immunoprecipitated from MCF-7 cells using a specific antibody for ERα. In the absence of estrogen, the protein complex purified from MCF-7 contained the same components as the complex in 293 cells (Figure 3C, right panel), suggesting that this protein complex exists in the physiological conditions.

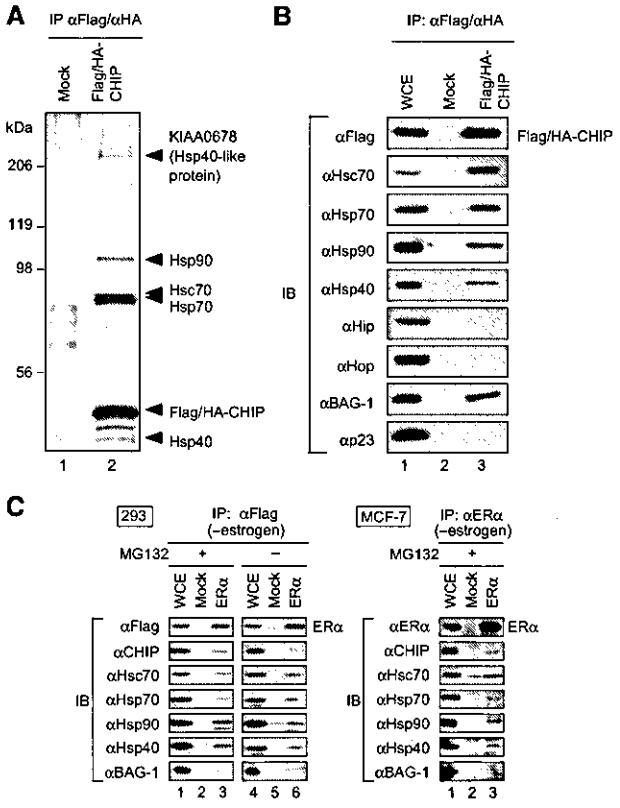

Figure 3 Purification and identification of a protein complex containing CHIP. (**A, B**) HeLa S3 cells (Mock) or HeLa S3 cells constitutively expressing Flag/HA double-tagged CHIP (Flag/HA-CHIP) were subjected to sequential immunoprecipitation using anti-Flag M2 and anti-HA antibody as described in Materials and methods. The purified fractions were subjected to SDS–PAGE followed by silver staining (A). Proteins eluted from these columns were examined by mass spectrometry (A) and Western blotting (B). Total HeLa cell extract is shown in lane 1 (WCE) (B). (**C**) Unliganded ERα interacted with a protein complex containing chaperones and CHIP. Flag-ERα-transfected 293 cells (ERα), untransfected cells (Mock) or MCF-7 cells were subjected to immunoprecipitation using either anti-Flag M2 (left panel) or anti-ERα (right panel) antibody and then Western blotted using indicated antibodies. The whole-cell extract is shown in lane 1 (WCE).

CHIP ubiquitinates and degrades unliganded ERα

To test whether CHIP is involved in the ubiquitination and degradation of unliganded ERα, either ERα or ERαΔAD was transfected into 293 cells with or without CHIP. Western blot analysis revealed that, in the absence of estrogen, the steady-state levels of ERα and ERαΔAD were decreased when CHIP was expressed (Figure 4A; 293, lanes 3 and 5). In contrast, in the presence of estrogen, the expression of CHIP exhibited little or no effect on the protein level of ERα and ERαΔAD (Figure 4A; 293, lanes 4 and 6). Endogenous ERα in MCF-7 cells was also decreased by CHIP expression (Figure 4A; MCF-7). Cell treatment with MG132 or lactacystin blocked CHIP-dependent ERα degradation, indicating that the degradation is mediated through proteasome pathways (Figure 4A, lower panel). We further determined the CHIP function by developing MCF-7 cells in which endogenous CHIP expression was suppressed by the introduction of a small interfering RNA (siRNA) complementary to sequences present in the CHIP mRNA. The introduction of the siRNA vector into MCF-7 cells resulted in the suppression of CHIP mRNA (data not shown) and protein expression, and the accumulation of ERα protein (Figure 4B). In contrast, a control vector failed to alter the CHIP or ERα protein level. In addition, either OHT or ICI treatment abrogated CHIP-induced ERα degradation (Figure 4C). Considering the observation that OHT- or ICI-bound ERα showed no interaction with CHIP, it is suggested that the degradation requires binding between ERα and CHIP.

To confirm that CHIP enhances unliganded ERα degradation, pulse-chase experiments were performed. In the absence of CHIP, the half-life of unliganded ERα exceeded 12 h (Figure 4D; 293), whereas, in the presence of CHIP, the turnover of unliganded ERα increased and exhibited a half-life of approximately 6 h (Figure 4D; 293). The half-life of estrogen-bound ERα was not changed by the expression of CHIP (data not shown). In MCF-7 cells, CHIP also enhanced the turnover of endogenous ERα in the absence of estrogen (Figure 4D; MCF-7). To test the specificity of this effect, we created constructs in which the TPR and U-box domains of CHIP were deleted (ΔTPR and ΔUbox). CHIP binds to Hsp/Hsc70 by means of its TPR motif, while also displaying E3 ubiquitin-ligase activity mediated by its U-box domain. Although the expression of these proteins was similar to that of wild-type CHIP (data not shown), the deletion of either of these domains abolished the effects of CHIP on ERα or ERαΔAD protein level (Figure 5A). The requirement of a TPR motif indicates that CHIP may need to interact with Hsc70 to promote ERα degradation. Functional requirement

of the U-box implies that CHIP regulates ERα ubiquitination. In order to validate this model, we evaluated the presence of Hsp/Hsc70 and ERα in complexes containing CHIPΔTPR or CHIPΔUbox. As shown in Figure 5B, CHIPΔTPR did not have the ability to form a complex with Hsc70 and ERα, indicating that Hsc70 mediates the interaction between ERα and CHIP. Finally, we tested whether CHIP enhances ERα turnover through ubiquitination. When ERα was coexpressed with CHIP, we observed the appearance of smeary bands of ubiquitin-conjugated ERα products (Figure 5C, lanes 3 and 5). In the presence of estrogen, CHIP did not enhance the conjugation of ubiquitin to ERα (Figure 5C, lanes 2 and 4). Overall, these observations indicate that the ubiquitination and degradation of unliganded ERα is mediated by a protein complex containing CHIP ubiquitin ligase.

CHIP preferentially recognizes and degrades misfolded ERα

To investigate the effect of CHIP on the transcriptional activity of ERα, a luciferase assay was performed as shown in Figure 6A. While the protein level of ERα was reduced by the expression of CHIP (Figure 6B, upper panel), the transcriptional activity of ERα was slightly enhanced by CHIP expression (Figure 6B, lower panel, compare lane 2 with lanes 5 and 8). Therefore, we next estimated the level of transcriptional activity per ERα protein amount. When ERα was coexpressed with CHIP, the level of transcriptional activity per ERα protein was about two-fold higher than ERα alone (Figure 6B, lower panel, compare lane 3 with lanes 6 and 9).

Our results show that CHIP binds to unliganded but not to liganded ERα. In addition, CHIP was localized mainly in the cytoplasm (Figure 6C). From these observations, it is difficult to believe that CHIP acts as a coactivator for ERα in the nucleus. Furthermore, ERα(HE82), which has three amino-acid substitutions in the DNA-binding region (C domain) in ERα and has almost no ability to bind DNA (Mader *et al*, 1989), was also degraded by CHIP, suggesting that the CHIP-dependent degradation of ERα does not require DNA binding. From these results and previous reports (Hohfeld *et al*, 2001; Meacham *et al*, 2001; Murata *et al*, 2001; Goldberg, 2003), we hypothesized that CHIP preferentially ubiquitinates misfolded ERα proteins to eliminate them. CHIP expression may selectively reduce the protein level of unfolded or misfolded ERα, which has less activity than the normal form. Consequently, CHIP could enhance the level of transcriptional activity per ERα protein.

To test this hypothesis, amino-acid substitutions were introduced into ERα to induce protein misfolding. In the absence of ligands, ERα(V364E) (McInerney *et al*, 1996)

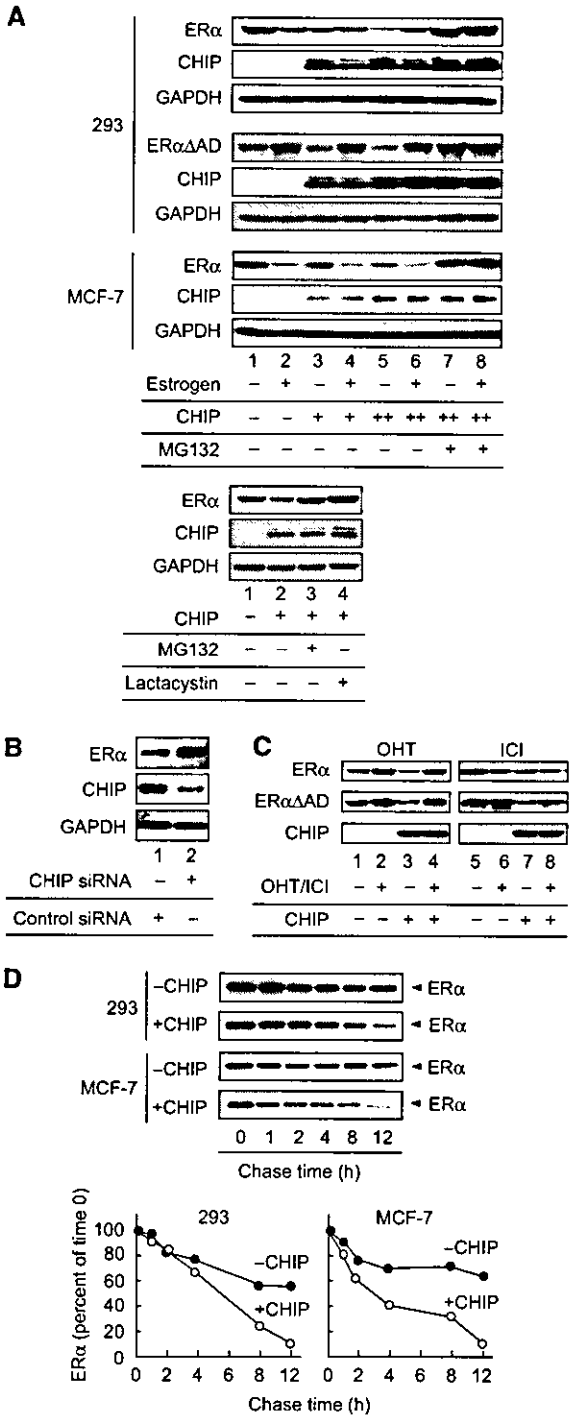

Figure 4 CHIP ubiquitinated and degraded unliganded ERα. **(A)** CHIP facilitated the degradation of unliganded ERα. HA-tagged CHIP (250 ng) was cotransfected into 293 or MCF-7 cells with or without ERα or ERαΔAD (500 ng) and in the absence or presence of estrogen (10^{-8} M), MG132 or lactacystin (10^{-6} M). The protein level of ERα was examined by Western blotting using anti-ERα antibody. **(B)** siRNA-mediated suppression of endogenous CHIP. The plasmid containing siRNA specific for CHIP or control vector was introduced into MCF-7 cells. Transfected cells were selected by puromycin. Protein levels of CHIP and ERα were assessed by immunoblotting of whole-cell lysate with the specific antibodies as indicated. **(C)** CHIP did not alter the steady-state level of ERα in the presence of OHT or ICI. Either ERα or ERαΔAD (500 ng) was cotransfected into 293 cells with or without HA-CHIP (250 ng) in the absence or presence of the indicated ligands. The protein level of ERα was examined by Western blotting using specific antibodies for ERα. **(D)** Pulse-chase assay. 293 cells transfected with CHIP (250 ng) and ERα (500 ng) or MCF-7 cells transfected with CHIP (2 μg) were pulse-labeled with [^{35}S]methionine and then chased for the indicated times in media containing unlabeled methionine. ^{35}S-labeled ERα in anti-ERα immunoprecipitate was quantified by phosphoimaging, and the levels in control cells (closed circle) and CHIP-expressing cells (open circle) were plotted relative to the amount present at time 0.

and ERα(C447A) (Reese and Katzenellenbogen, 1992), both of which have an amino-acid substitution in the LBD and exhibit temperature sensitivity, were unstable and degraded faster than wild-type protein at a nonpermissive temperature (37°C). Wild-type ERα also degraded to the same extent as temperature-sensitive mutants when cells were cultured under thermally stressed conditions (cells were cultured at 42°C for 30 min) (Figure 6D, upper panel, compare lane 1 with lanes 2, 3 and 6). In contrast, ERα(L540Q) (Ince *et al*, 1995) and ERαΔAD, which have either an amino-acid substitution or truncation in the flexible Helix 12 region, exhibited the same stability as wild type at 37°C (Figure 6D, upper panel, compare lane 1 with lanes 4 and 5). Under a permissive temperature (30°C), the protein stability of ERα(V364E) and ERα(C447A) was comparable with that of the wild type (Figure 6D, lower panel).

In a luciferase assay, these four mutated ERα proteins showed a loss or reduction of transcriptional activity compared to the wild type (Figure 6E, lane 5), and they were able to suppress wild-type activity when coexpressed with wild-type ERα (Figure 6E, lane 8). CHIP did not enhance the ERα activity suppressed by ERα(L540Q) or ERαΔAD; however, transcriptional activity suppressed by ERα(V364E) or ERα(C447A) was recovered by CHIP expression (Figure 6E, lanes 9 and 10). These results suggest that CHIP may preferentially ubiquitinate ERα(V364E) and ERα(C447A) to degrade these mutants.

If CHIP is directly involved in the hydrolysis of abnormal or mutant forms of ERα, then it should be able to form specific complexes with mutated or misfolded ERα. ERα or mutated forms of ERα were immunoprecipitated from transfected cells and the presence of CHIP and chaperone proteins was detected using specific antibodies. At a permissive temperature (30°C), the amount of CHIP in the precipitate pellets with ERα(V364E) or ERα(C447A) was almost the same in precipitates with the wild type (Figure 7A, right panel). However, at a nonpermissive temperature (37°C), CHIP and BAG-1, a co-chaperone that binds to both Hsc70 and the proteasome, preferentially co-immunoprecipitated with ERα(V364E) and ERα(C447A), while the amount of other chaperone components in precipitants was unchanged (Figure 7A, left panel). In addition, thermally stressed conditions (42°C for 30 min) also increased the CHIP and BAG-1 levels in the precipitated pellet (Figure 7A, left panel, lane 6). Consistent with the results obtained from the degradation and interaction experiments, the polyubiquitination of the temperature-sensitive mutants or thermally denatured ERα was enhanced at nonpermissive temperature (Figure 7B, compare left panel with right panel).

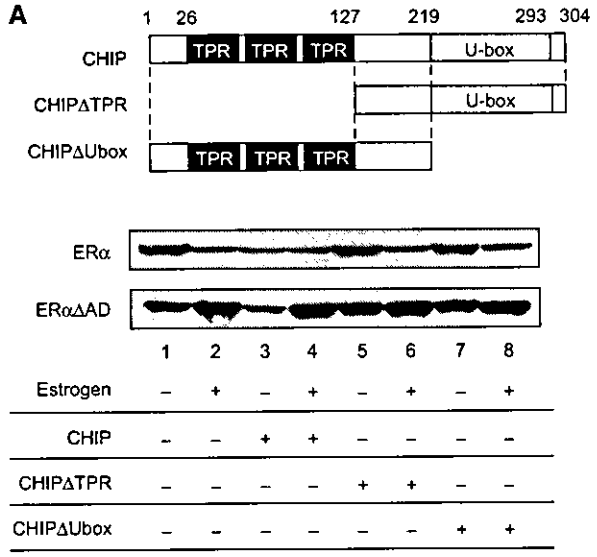

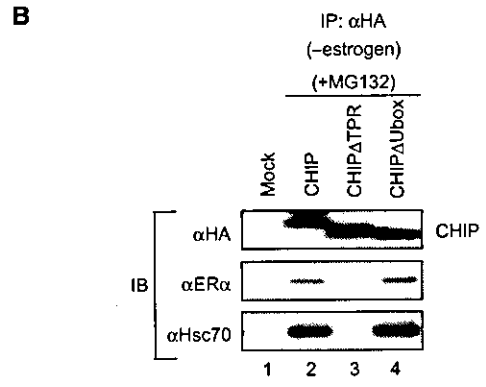

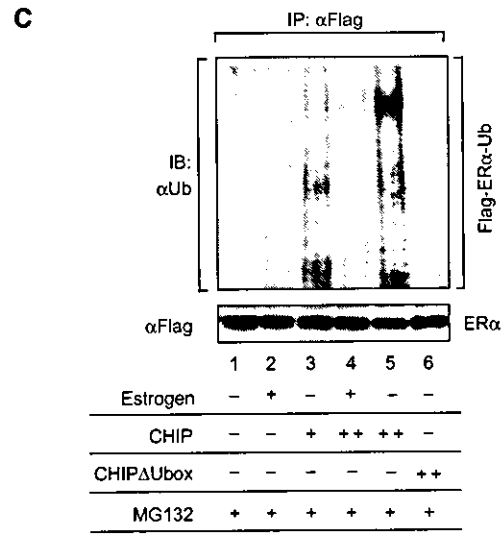

Liganded but not unliganded ERα degradation is observed in CHIP–/– cells

To firmly establish the importance of the observation of CHIP-dependent ERα degradation, we isolated mouse embryonic

Figure 5 CHIP-dependent ubiquitination and degradation of ERα required its TPR and U-box domain. (**A**) Both the TPR and U-box domain in CHIP were necessary for ERα degradation. CHIP, CHIPΔTPR or CHIPΔUbox (250 ng) was transfected into 293 cells with or without ERα or ERαΔAD (500 ng). Protein levels of ERα and ERαΔAD were examined by Western blotting using anti-ERα antibody. (**B**) The TPR domain of CHIP is necessary for binding to Hsc70 and ERα. HA-tagged CHIP or CHIP mutants were expressed in 293 cells and immunoprecipitated with anti-HA antibody in the absence of estrogen. Precipitates were Western blotted with antibodies for CHIP, ERα and Hsc70. (**C**) CHIP induced the ubiquitination of unliganded ERα. Flag-tagged ERα (500 ng) was transfected into 293 cells with or without CHIP (250 ng) or CHIPΔUbox (250 ng) in the presence or absence of estrogen (10^{-8} M). Flag-tagged ERα was immunoprecipitated using anti-Flag M2 antibody. The ubiquitination status of ERα was analyzed by Western blotting using anti-ubiquitin antibody.

fibroblast (MEF) cells from either CHIP−/−, CHIP+/− mice or wild-type littermates, CHIP+/+, and determined the protein level of ERα. To induce misfolding of ERα protein, these cells were cultured under thermally stressed conditions. In the absence of estrogen, the thermally stress conditions reduced ERα levels in both CHIP+/+ and CHIP+/− cells but not in CHIP−/− cells (Figure 8A, lanes 4–6). MG132 induced the accumulation of ERα in CHIP+/+ and CHIP+/− cells, indicating that ERα was degraded through proteasome pathways in these cells. These observations provide further support for a model in which CHIP preferentially binds misfolded ERα proteins and degrades them to maintain the quality of ERα protein in cells. Co-immunoprecipitation experiments showed the existence of ERα/Hsc70/CHIP complex in CHIP+/+ cells but not in CHIP−/− cells (Figure 8B). Furthermore, estrogen treatment induced ERα degradation in CHIP−/− cells to the same extent as in CHIP+/+ cells (Figure 8C), suggesting that CHIP is not involved in estrogen-dependent degradation, and supporting the idea that there are two independent ubiquitin–proteasome pathways for ERα (Figure 8D).

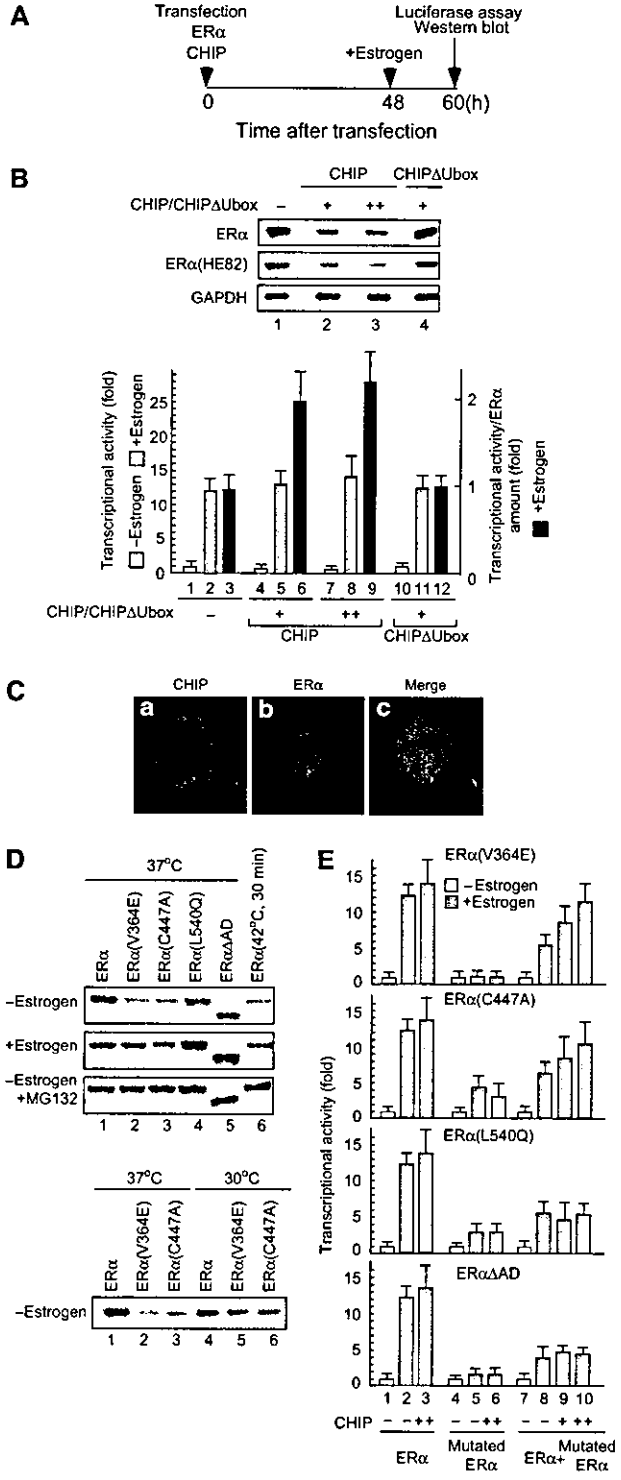

Discussion

Estrogen receptor α is regulated by two independent ubiquitin–proteasome pathways

Several studies have mentioned that the AD core region of ERα is essential not only for transactivation but also for estrogen-dependent ERα degradation (Lonard *et al*, 2000). These reports are in good agreement with our result that ERαΔAD, which has no AD core region, does not show estrogen-dependent degradation. Interestingly, however, MG132 had no effect on ligand-bound ERαΔAD; the steady-state level of ERαΔAD in the absence of estrogen is accumulated in the presence of MG132. These results indicate that unliganded ERαΔAD is still degraded through proteasome pathways. According to these observations, it is possible that the degradation pathway for the unliganded receptor differs from that for liganded. ERαΔAD might be able to recruit a

Figure 6 CHIP preferentially recognized and degraded misfolded ERα. (**A**) The time schedule for luciferase assay and Western blot analysis. 293 cells were transfected with indicated plasmids. At 48 h after transfection, cells were treated with estrogen (10^{-8} M) for an additional 12 h and harvested for luciferase assay and Western blotting. (**B**) The level of transcriptional activity per ERα protein amount was enhanced by CHIP. Upper panel: The steady-state level of ERα or ERα(HE82) was reduced by the expression of CHIP but not by CHIPΔUbox. Lower panel: Transcriptional activity of ERα was slightly enhanced by CHIP. ERα (100 ng) and either CHIP or CHIPΔUbox (100 ng) were cotransfected into 293 cells with ERE-TATA-Luc (100 ng) and pRSVβGAL (100 ng), and cell extracts were used in a luciferase assay. The protein amount of ERα was quantified by phosphoimaging. The levels of transcriptional activity per ERα protein amount were plotted relative to the level in control cells. (**C**) Immunocytochemistry of CHIP and ERα. 293 cells were transiently transfected with HA-tagged CHIP and ERα. The mounted cells were examined by immunofluorescence microscopy as described in Materials and methods. Green represents immunofluorescence for HA-CHIP and red ERα. The distribution of CHIP in a cell body is shown in panel a, and panel b shows the distribution of ERα. Panel c shows the merge images of panels a and b. (**D**) Temperature-sensitive mutants of ERα degraded faster than wild-type ERα in the absence of ligands. ERα(V364E), ERα(C447A), both of which are temperature sensitive, and ERα(L540Q) were generated by amino-acid substitutions of wild-type ERα. Indicated ERα or ERα mutants (500 ng) were transfected into 293 cells in the presence or absence of estrogen (10^{-8} M) and MG132 (10^{-6} M) at 30°C (permissive temperature; lower panel), 37°C (normal/nonpermissive temperature; upper panel) or under thermally stressed conditions (42°C for 30 min; upper panel). Protein levels of ERα or mutants were analyzed by Western blotting using anti-ERα antibody. (**E**) CHIP recovered the transcriptional activity of ERα suppressed by coexpression of ERα mutants. ERα (100 ng), ERE-TATA-Luc (100 ng) and pRSVβGAL (100 ng) were cotransfected into 293 cells with or without either ERα(V364E), ERα(C447A), ERα(L540Q), ERαΔAD (100 ng) or CHIP (100 ng), and cell extracts were used in a luciferase assay.